JOURNAL OF GEOPHYSICAL RESEARCH, VOL. 111, E11010, doi:10.1029/2006JE002714, 2006

Geologic constraints on crustal plateau surface histories, Venus: The lava pond and bolide impact hypotheses

Vicki L. Hansen[1]

Received 10 March 2006; revised 6 July 2006; accepted 11 July 2006; published 22 November 2006.

[1] Venusian crustal plateau formation is hotly debated. Crustal plateaus are large (~1500–2500 km) quasi-circular ~0.5- to 4-km-high plateaus that host distinctive tectonic fabrics, called ribbon tessera. Debate centers on plateau support and fabric formation. Detailed geologic mapping of an ~360,000 km^2 region, eastern Ovda Regio, provides critical clues for plateau evolution. Ribbon-tessera fabrics record broadly synchronous layer contraction, extension, and flooding, as an initially strong, thin layer (<100 m) developed across Ovda. As the layer underwent ductile shortening and brittle extension, subsurface lava flooded structural lows. With progressive deformation the layer thickened, leading to formation of progressively longer-wavelength structures. Early-formed shorter-wavelength structures and lava- filled valleys were carried piggyback on longer-wavelength folds. This history indicates an extremely large strength contrast that is inconsistent with a conductive geotherm, reflecting instead the presence of a near-surface molten layer. I propose the lava-pond hypothesis: Ribbon-tessera fabrics represent progressively solidified "scum" of a huge lava pond, leading to crustal plateau formation. I further propose that individual lava ponds formed as a result of large bolide (~20–30 km diameter) impact with ancient thin lithosphere, causing massive partial melting in the upper mantle. Melt rose buoyantly to form huge (~1500–2000 km diameter) lava ponds, completely resurfacing the local area. In the upper mantle depleted residuum would be compositionally more buoyant and stronger than adjacent undepleted mantle. Isostatic adjustment resulted in pond uplift and plateau formation. Subsequent secular cooling could "freeze" a plateau in place, or mantle convection could strip away the residuum root, leading to plateau collapse.

Citation: Hansen, V. L. (2006), Geologic constraints on crustal plateau surface histories, Venus: The lava pond and bolide impact hypotheses, *J. Geophys. Res.*, *111*, E11010, doi:10.1029/2006JE002714.

1. Introduction

[2] Venusian crustal plateau formation is one of the most hotly debated topics to emerge from NASA's Magellan Mission. Crustal plateaus, 1500–2500 km diameter quasi-circular plateaus that rise 0.5 to 4 km above surrounding terrain, host distinctive deformation fabrics called ribbon tessera. Scientists generally agree that thickened crust supports crustal plateaus, as evidenced by small gravity anomalies, low gravity to topography ratios, and shallow apparent depths of compensation (ADC) [*Smrekar and Phillips*, 1991; *Bindschadler et al.*, 1992a; *Grimm*, 1994a; *Phillips and Hansen*, 1994; *Bindschadler*, 1995; *Simons et al.*, 1997; *Hansen et al.*, 1997]. The spatial correlation of crustal plateau topography and tectonic fabrics strongly suggests that thickening and surface deformation are genetically related [*Bindschadler and Head*, 1991; *Bindschadler et al.*, 1992a, 1992b; *Bindschadler*, 1995; *Hansen and Willis*, 1996, 1998; *Ghent and Hansen*, 1999; *Hansen et al.*, 1999, 2000]. Researchers also widely accept that arcuate-shaped inliers of ribbon-tessera terrain that outcrop across expanses of Venus' lowland represent remnants of collapsed crustal plateaus [e.g., *Bindschadler et al.*, 1992b; *Phillips and Hansen*, 1994; *Bindschadler*, 1995; *Ivanov and Head*, 1996; *Hansen et al.*, 1997; *Hansen and Willis*, 1998; *Ghent and Tibuleac*, 2002].

[3] The crustal plateau debate centers on uncertainties about the crustal thickening mechanism and formation of the distinctive tectonic fabrics. Two end-member explanations have emerged: downwelling and plume hypotheses. The downwelling hypothesis involves concurrent crustal thickening and surface deformation due to subsolidus flow and horizontal lithospheric accretion associated with a cold mantle diapir beneath ancient thin lithosphere [e.g., *Bindschadler and Parmentier*, 1990; *Bindschadler and Head*, 1991; *Bindschadler et al.*, 1992a, 1992b; *Bindschadler*, 1995; *Gilmore and Head*, 2000]. The plume hypothesis accommodates thickening and deformation via magmatic underplating and vertical accretion due to interaction of ancient thin lithosphere with a large thermal mantle plume [*Hansen*

[1]Department of Geological Sciences, University of Minnesota at Duluth, Duluth, Minnesota, USA.

0148-0227/06/2006JE002714$09.00

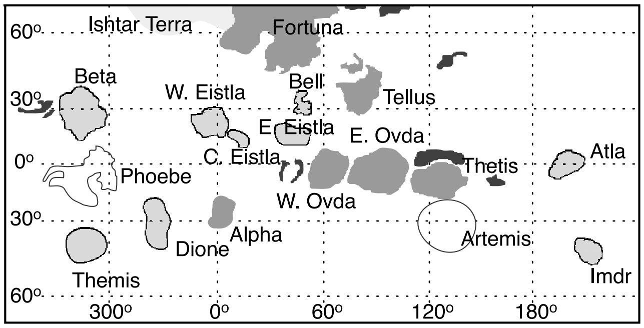

Figure 1. Cylindrical projection of Venus showing the location of crustal plateaus (dark gray), volcanic rises (light gray) and some of the large arcuate ribbon-tessera terrain inliers (black). Artemis and Phoebe Regio, which differ from both crustal plateaus and volcanic rises are show in white with black outline.

et al., 1997; *Hansen and Willis*, 1998; *Phillips and Hansen*, 1998; *Ghent and Hansen*, 1999; *Hansen et al.*, 1999, 2000].

[4] Both hypotheses call for time-transgressive deformation of ancient thin lithosphere above individual localized regions, and both accept the premise that arcuate ribbon-tessera terrain inliers represent collapsed crustal plateaus due to lower crustal flow following plateau formation. The first supposition seems robust. However, recent finite-element modeling indicates that the range of preserved crustal plateau morphologies and arcuate ribbon-tessera terrain inliers is difficult to achieve by collapse through lower crustal flow [*Nunes et al.*, 2004], challenging the second, widely held premise. Thus the range in elevations of plateaus and collapse mechanism remains unaddressed by either hypothesis.

[5] Geologic mapping conducted by workers on both sides of the debate agree that plateaus host multiple wavelengths of both extensional structures (ribbons, extensional troughs, and graben) and contractional structures (folds), and that low-viscosity fluid, presumably lava, fills local to regional topographic lows. Despite this agreement, controversy exists as to (1) the relative timing of flooding and deformation, and (2) the relative timing of extensional and contractional structures. In addition, estimates of the nature and amount(s) of layer shortening accommodated by short-wavelength folds are unconstrained, although such data should provide critical constraints for hypothesis evaluation.

[6] This contribution investigates the surface evolution of a 6° by 6° region (~360,000 km^2) of a crustal plateau, eastern Ovda Regio, in order to better understand: (1) the evolution of contractional structures, (2) kinematic relations between contractional and extensional structures, and (3) the timing of flooding relative to deformation and plateau evolution. Contractional structures that record significant strain might be difficult to address within the plume hypothesis, whereas surface flooding might pose a challenge to the downwelling hypothesis. This study yields new observations and refined geologic surface histories for eastern Ovda Regio. Eastern Ovda records broadly synchronous surface layer contraction, surface layer extension, and localized flooding by low-viscosity lava. The surface history and resulting constraints on rheology require a sharp decrease in viscosity with depth between the deforming surface layer and subsurface material. The surface layer must have been able to shorten in a ductile fashion yet extend in a brittle fashion, and subsurface material must have had an extremely low viscosity and an ability to flood structural lows formed within the surface layer. Collectively these observations call for the presence of liquid subsurface material, likely, silicate magma. This condition, taken together with the layer's ability to both fold in a ductile fashion and extend in a brittle fashion, indicates that eastern Ovda Regio records an extremely hot environment of formation. These results are difficult to reconcile with either the downwelling or the plume hypotheses as currently proposed. A third hypothesis emerges to explain the origin of crustal plateaus by formation of large-scale lava ponds. In this contribution I present new data that constrains the surface history of eastern Ovda Regio, and propose the lava-pond hypothesis of crustal plateau formation. I further propose that lava ponds record large bolide impact.

2. Background

[7] Venus, commonly referred to as Earth's sister planet, differs from Earth in many ways. Long linear highs and lows, characteristic features of plate tectonic processes, dominate Earth's global surface fabric, whereas circular to quasi-circular features, preserved across a huge size range, characterize Venus. Venus' quasi-circular features include, from smallest to largest: (1) hundreds of thousands of small shield edifices (1–20 km diameter, generally <10 km), (2) ~970 "pristine" impact craters (2–270 km diameter), (3) many small to large volcanic constructs (tens to hundreds of kilometers in diameter), (4) ~500 coronae (60–600 km diameter), (5) a few very large coronae (Artemis, Heng-o, Quetzalpetlatl, Atahensik) that might represent plume signatures [e.g., *Smrekar and Stofan*, 1997; *Hansen*, 2002, 2003, 2006b; *Ivanov and Head*, 2003] and (6) approximately equal numbers of volcanic rises and crustal plateaus, each less than ten in number (Figure 1).

[8] Volcanic rises and crustal plateaus, 1500- to 2500-km-diameter quasi-circular features, are similar in planform, but differ in: (1) topographic expression, (2) gravity-topography ratios and ADCs, and (3) geologic history. Volcanic rises are domical whereas crustal plateaus, in keeping with their name, display steep sides and flat tops. Deep ADCs for rises (~100–300 km) are taken as evidence of contemporary thermal support, whereas shallow ADCs for crustal plateaus (<100 km and typically <50 km) are generally interpreted as evidence of thickened crust providing isostatic support [*Smrekar and Phillips*, 1991; *Bindschadler et al.*, 1992a; *Grimm*, 1994a; *Phillips and Hansen*, 1994; *Bindschadler*, 1995; *Simons et al.*, 1997; *Hansen et al.*, 1997]. Volcanic rises are interpreted as the surface expression of large thermal mantle plumes on contemporary thick (~100 km) lithosphere [e.g., *Phillips et al.*, 1991; *McGill*, 1994; *Phillips and Hansen*, 1994; *Smrekar et al.*, 1997; *Nimmo and McKenzie*, 1998]. The genesis of crustal plateaus is debated.

[9] Six crustal plateaus, from north to south, occur on Venus: Fortuna, Tellus, western Ovda, eastern Ovda, Thetis, and Alpha (Figure 1). Phoebe, although considered by some as a crustal plateau [e.g., *Hansen et al.*, 1997], shows

geophysical characteristics hybrid between plateaus and rises [*Grimm*, 1994a; *Simons et al.*, 1997; *Kiefer and Peterson*, 2003] and its structural fabric is unique, and quite different from that of crustal plateaus [*Hansen and Willis*, 1996]. Crustal plateaus host distinctive deformation fabrics [*Bindschadler et al.*, 1992a; *Ivanov and Head*, 1996] called ribbon-tessera terrain [*Hansen and Willis*, 1996, 1998], and rise 0.5–4 km above the adjacent lowland. Spatial correlation of plateau topography with deformation fabrics suggests a genetic relationship between the thickening mechanism and surface deformation [*Bindschadler et al.*, 1992a, 1992b; *Bindschadler*, 1995; *Brown and Grimm*, 1997; *Ghent and Hansen*, 1999; *Hansen et al.*, 1997, 1999]. Inliers of characteristic ribbon-tessera terrain that outcrop within the lowland are widely accepted as remnants of ancient collapsed crustal plateaus [e.g., *Bindschadler et al.*, 1992b; *Phillips and Hansen*, 1994; *Bindschadler*, 1995; *Ivanov and Head*, 1996; *Hansen and Willis*, 1998; *Ghent and Tibuleac*, 2002], and the formation of these features must be considered by any viable hypothesis. In the case of arc-shaped inliers, fold crests commonly parallel the arcuate shape with ribbon fabrics trending orthogonal to the fold crests.

[10] The crustal plateau debate centers on the process responsible for crustal thickening and concurrent development of ribbon-tessera terrain tectonic fabrics. Downwelling calls for thickening by subsolidus flow and horizontal lithospheric accretion of ancient thin lithosphere associated with a focused cold mantle downwelling [*Bindschadler and Parmentier*, 1990; *Bindschadler et al.*, 1992a, 1992b; *Bindschadler*, 1995; *Brown and Grimm*, 1997]. Contractional strain should dominate surface deformation in this case, which should have been accompanied by a relatively cold geothermal gradient. The plume hypothesis calls for thickening via magmatic underplating and vertical accretion due to interaction of ancient thin lithosphere with a large thermal mantle plume [*Hansen et al.*, 1997; *Phillips and Hansen*, 1998; *Hansen and Willis*, 1998; *Hansen et al.*, 1999, 2000; *Ghent and Hansen*, 1999]. A hot geothermal gradient should accompany deformation, which might have both extensional and contractional components, although large amounts of contractional strain would be inconsistent with, or challenging to address within the context of, the plume hypothesis.

[11] As noted, both hypotheses embrace the premise that thickened crust forms the crustal plateau root and that “collapsed” crustal plateaus result from the loss of this root. However, finite element modeling [*Nunes et al.*, 2004] illustrates that the range of preserved crustal plateau morphologies and arcuate ribbon-tessera terrain inliers is difficult to achieve through lower crustal flow at geologically reasonable timescales. These results present a challenge to the widely held premise that collapsed plateaus result from the loss of a crustal root. Thus, although both the downwelling and the plume hypotheses call for lower crustal flow to accommodate the range in plateau and inlier topography, collapse by lower crust flow might not be viable, or it may be that parameters employed by the collapse model are inappropriate. Regardless, the range in elevations of plateaus and inliers currently remain unaddressed by either the downwelling or the plume hypothesis.

[12] In addition, neither the downwelling nor the plume hypotheses address all characteristics of crustal plateaus, and each hypothesis has specific problems. Challenges for the downwelling hypothesis include: (1) a predicted domical shape rather than the observed plateau shape [*Bindschadler and Parmentier*, 1990; *Kidder and Phillips*, 1996]; (2) lower crustal flow called upon for crustal thickening requires 1–4 billion years, well outside the absolute time constraints allowed by geologic relations [*Kidder and Phillips*, 1996]; and (3) formation of documented short-wavelength extensional structures (ribbon fabrics) is difficult to explain in the cold downwelling environment [*Hansen and Willis*, 1998; *Hansen et al.*, 2000]. The plume hypothesis can accommodate formation of a plateau shape and extensional features in a viable timeframe [*Hansen and Willis*, 1998; *Hansen et al.*, 1999, 2000]; however, extensive contractional strain could be difficult to accommodate within the plume hypothesis. Although the plume hypothesis addresses formation of late long-wavelength folds (or warps), which record very little (<1%) shortening [*Ghent and Hansen*, 1999], early layer shortening and/or large amounts of layer shortening would present a serious challenge for the plume hypothesis [*Ghent et al.*, 2005]. In addition, *Gilmore et al.* [1998] argued that formation of ribbon-tessera terrain requires a geothermal gradient much in excess of what might be achieved in a plume-lithosphere interaction environment.

[13] Despite disagreement about crustal plateau formation, geologic mapping by many workers leads to four, mutually agreed upon, observations: (1) plateaus host both contractional structures (folds) and extensional structures (ribbons, extensional troughs, graben); (2) multiple suites of folds occur, distinguished by wavelength; (3) multiple suites of extensional structures occur, defined by their spacing (or wavelength); and (4) low-viscosity fluid, presumably lava, filled local to regional topographic lows [e.g., *Bindschadler et al.*, 1992a; *Bindschadler*, 1995; *Hansen and Willis*, 1996, 1998; *Gilmore et al.*, 1998; *Ghent and Hansen*, 1999; *Hansen et al.*, 1999, 2000; *Banks and Hansen*, 2000]. Despite these commonalities, debate exists as to (1) the timing of flooding relative to deformation, and (2) the relative timing of contractional and extensional structures.

[14] The crustal plateau flooding controversy can be summarized as: (1) did flooding generally postdate deformation, and as such was likely genetically unrelated to crustal plateau formation [e.g., *Gilmore et al.*, 1997, 1998; *Basilevsky and Head*, 1998; *Head and Basilevsky*, 1998; *Gilmore and Head*, 2000]; or (2) did flooding accompany surface deformation, and was therefore genetically related to crustal plateau formation [e.g., *Banks and Hansen*, 2000]? The relative timing of contractional versus extensional structures depends, at least in part, on documenting various structural wavelengths and the mechanism(s) responsible for the formation of multiple-wavelength structures. Proponents of both the downwelling and the plume hypotheses agree that plateaus host late extensional strain in the form of spaced, lens-shaped (plan view), complex graben, which can be accommodated by either hypothesis. However, short-wavelength extensional structures (ribbon fabrics) might be accommodated by the plume hypothesis, but not the downwelling hypothesis. If ribbon-tessera terrain formation requires an extremely high geothermal gradient [e.g., *Gilmore et al.*, 1998], then ribbon fabric formation may

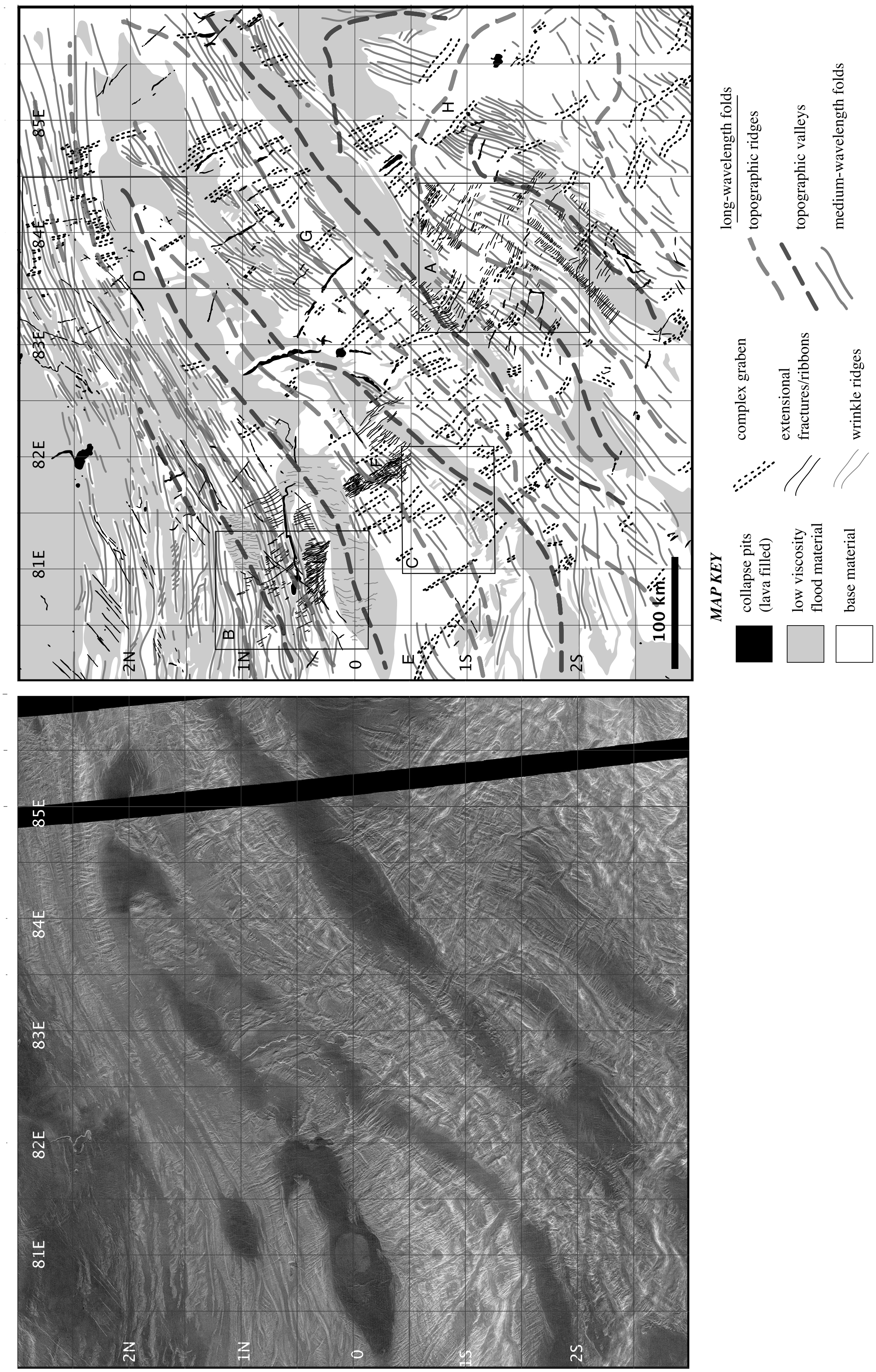
81E
82E
83E
84E
85E
2N
1N
0
1S
2S
A
B
C
D
E
F
G
H
100 km
MAP KEY
collapse pits (lava filled)
low viscosity flood material
base material
complex graben
extensional fractures/ribbons
wrinkle ridges
long-wavelength folds
topographic ridges
topographic valleys
medium-wavelength folds

Figure 2

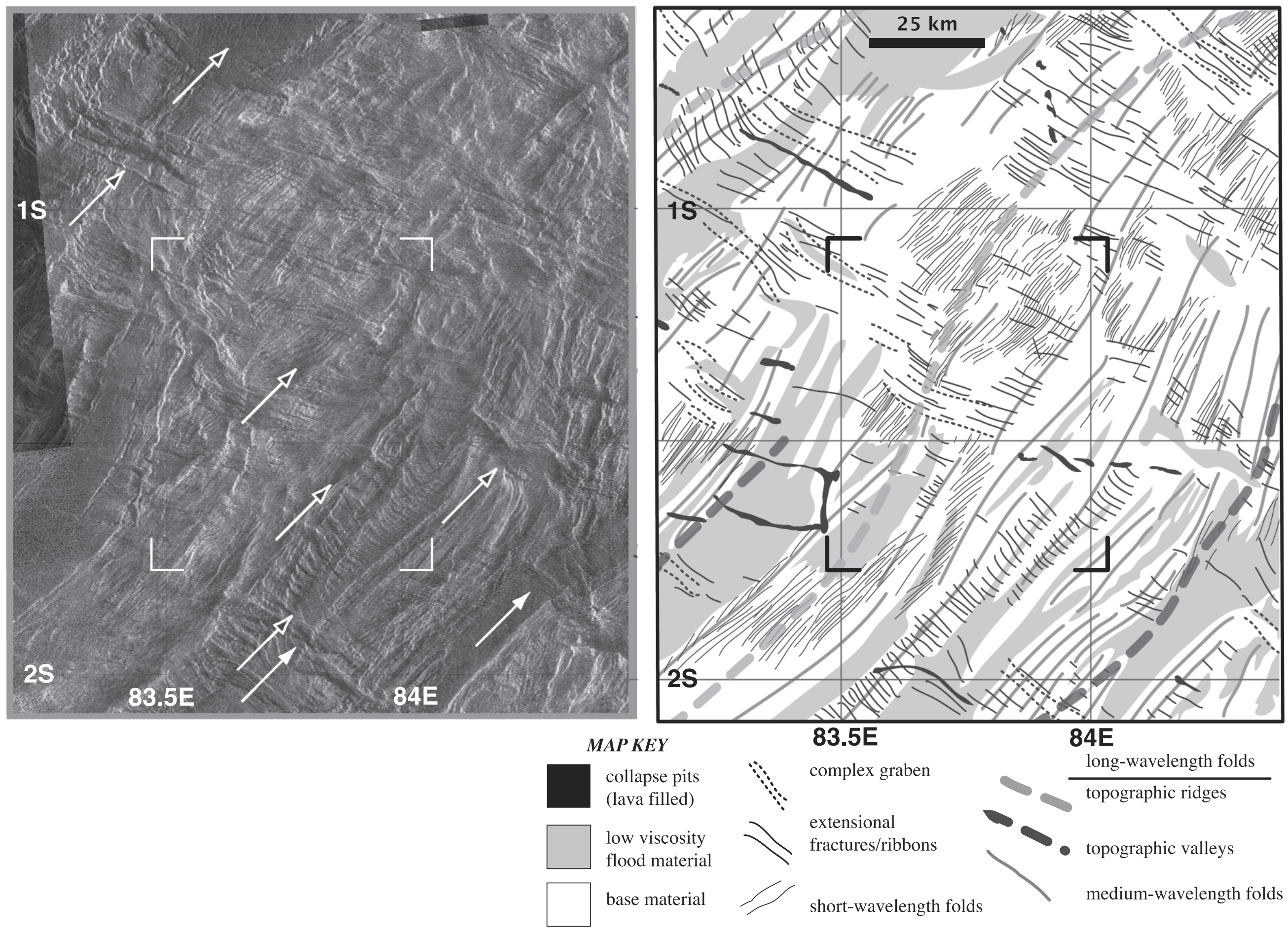

Figure 3. Left-illumination SAR image and geologic map of location A along the crest of a long-wavelength fold (see Figure 2 for location). Folds trend NE and extensional structures trend NW; short-wavelength folds have wavelength <0.6 km (image effective resolution); short-wavelength and medium-wavelength folds occur along the crest, limb and trough of long-wavelength folds; extensional structures cut folds and are deformed by folds. Local structural lows are filled with low-viscosity (flood) material; black head arrows indicate where flooding postdated local deformation; white head arrows indicate where deformation postdated flooding. White angles indicate region of Figure 4 detail.

prove challenging for both the downwelling and plume hypotheses. Whereas both hypotheses can account for small amounts of late shortening exemplified by long-wavelength folds, occurrence of short-wavelength folds could also prove challenging for both hypotheses depending on the amount and mechanism of shortening [*Ghent et al.*, 2005]. This contribution focuses on understanding the formation of short-wavelength features, particularly folds, and the timing of surface flooding relative to surface deformation. The formation of short-wavelength extensional structures (ribbons) is addressed in detail elsewhere [*Hansen and Willis*, 1996, 1998; *Pritchard et al.*, 1997; *Ghent and Hansen*, 1999; *Hansen et al.*, 2000; *Ghent and Tibuleac*, 2002].

3. Data and Methodology

[15] I explore the nature and relative timing of surface fabric development and flooding through detailed mapping and geological analysis of a 6° by 6° region (~360,000 km^2) of eastern Ovda Regio (centered at 0°N, 83°E) with the explicit goal of answering two questions. (1) What is the nature of the short-wavelength contractional structures

Figure 2. Left-illumination SAR image and geologic map of part of the northern Ovda Regio, 0N/83E study area. Long-wavelength fold trends determined from altimetry data. Note parallelism of multiple-wavelength contractional structures, orthogonal extensional structures (also of multiple wavelength), and widespread flooding of local structural lows independent of basin position on long-wavelength fold troughs, limbs or crests, although largest flood basins occur in long-wavelength fold troughs. Locations of detailed study areas A-H shown by boxes and/or letters. Locations E (~0.5S/80.5E) and F (~0.25S/82E).

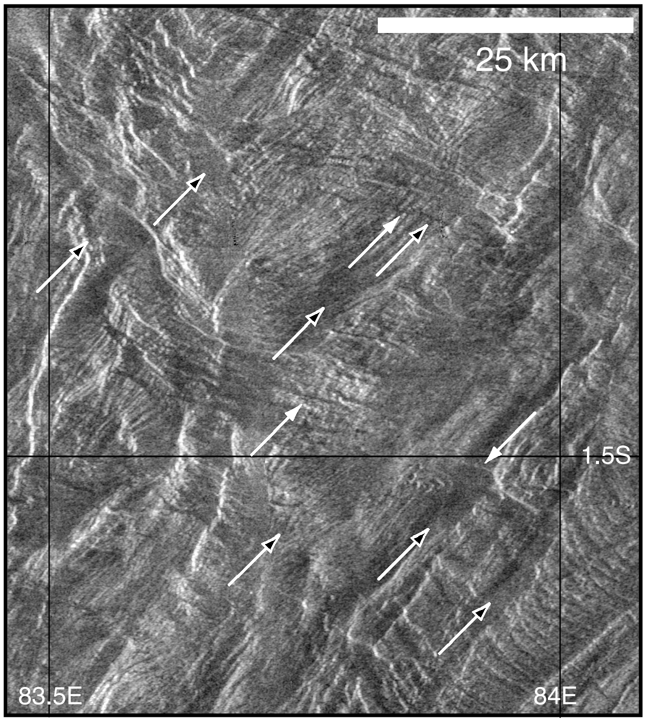

Figure 4. Left-illumination SAR image of area indicated in Figure 3. Black head arrows indicate where flooding postdated deformation; white head arrows indicate where deformation postdated local flooding.

(folds), including their range of wavelengths, spatial distribution, orientation, and relative timing with respect to other fold suites and with respect to extensional structure formation? (2) What is the timing of local flooding relative to tectonic fabric development? Specifically, it is important to determine whether flooding generally postdated deformation (likely unrelated to plateau formation) or accompanied deformation (likely related to plateau formation)?

[16] Answers to these questions are addressed by detailed geologic mapping using NASA *Magellan* S-band synthetic aperture radar (SAR) imagery and altimetry data. Data include: (1) compressed "C1" (~225 m/pixel) SAR data, (2) full-resolution "F" (75–100 m/pixel) SAR imagery of both right- and left-illumination data, (3) full-resolution true stereo SAR images constructed following *Plaut* [1993], (4) *Magellan* altimetry (~8 km along-track by 20 km across-track footprint with ~30-m average vertical accuracy which improves to ~10 m in smooth areas [*Ford et al.*, 1993]), and (5) synthetic stereo images constructed following *Kirk et al.* [1992] using NIH-Image macros developed by D.A. Young. *Magellan* SAR images were downloaded from the USGS Map-a-Planet website. All images were viewed in both normal and inverted (negative) modes to highlight structural details; lineaments are typically more apparent in inverted images. In addition, copies of images were stretched with a high contrast to accentuate lineaments in order to determine structural wavelength. SAR image interpretation follows *Ford et al.* [1993]; mapping follows guidelines and cautions of *Wilhelms* [1990], *Tanaka et al.* [1994], *Hansen* [2000], and *Zimbelman* [2001]. The major observations and implications that emerged from mapping are discussed in turn.

4. Observations

4.1. Mapping

[17] Figure 2 illustrates the study area (herein referred to as 0N83E) and the geologic map. Northeast-trending folds with wavelengths 75–150 km define the northwestern edge of eastern Ovda Regio, and they parallel the northwestern plateau margin with the adjacent lowland. Radar-smooth regions, presumably marked by solidified lava, define the broad axial fold troughs; fold troughs and crests, delineated in altimetry data, generally show elevation differences of 1–1.5 km. Extensional structures, which trend normal to the fold crests, define two morphologies: (1) parallel, paired radar bright- and dark-lineaments define a periodic fabric marked by parallel extensional troughs and ridges with large length:width aspect ratios, termed ribbon fabrics (see *Hansen and Willis* [1998] for detailed discussion of ribbon fabrics); and (2) extensional troughs with generally smaller aspect ratios and spaced more broadly than ribbon fabrics, which describe lens-shaped zones in plan view interpreted as complex graben (see *Ghent and Hansen* [1999] for detailed discussion of Ovda structures). Graben trend parallel to ribbon fabrics. Close examination of SAR images also reveals a range of fold wavelengths (Figure 3). Short- and medium-wavelength folds occur along the crests, limbs, and troughs of long-wavelength folds. Collapse pits or pit chains [e.g., *Okubo and Martel*, 1998; *Mege et al.*, 2003] also occur variably across the map area. In general pit chains broadly parallel extensional fabrics, although pit chain orientation deviates locally from that of extensional structures. Local flooding, marked by low radar backscatter, completely buries fold troughs and crests, as well as orthogonal extensional troughs and ridges. In some cases extensional structures clearly cut radar-smooth "flood" surfaces. Locally wrinkle ridges, which generally parallel adjacent extensional structures, cut smooth flood surfaces, indicating limited contraction of the flood layer and likely inversion or reactivation of earlier formed structures [e.g., *DeShon et al.*, 2000]. Detailed mapping in three locations reveals critical clues about the character and evolution of the deformation fabrics, as discussed in turn below.

4.1.1. Location A

[18] Location A (Figure 3) includes the crest (~6055 km) and trough (~6054.2 km) of a prominent fold. Along the fold crest, the highest local elevation, medium- and short-wavelength folds trend parallel to the long-wavelength fold crest. Orthogonal ribbon fabrics locally disrupt short- to medium-wavelength folds; complex graben, which parallel ribbon trends, cut long-wavelength folds. All folds trend broadly parallel to one another whereas extensional structures (ribbons and complex graben) parallel one another, and consistently trend orthogonal to fold trends. Medium-wavelength folds are apparent in Figures 3 and 4. In Figure 4, short-wavelength folds trend northeast parallel to long-wavelength folds. Locally, fold troughs of both short- and medium-wavelength folds are radar smooth, presumably the result of local flooding by low-backscatter, low-viscosity

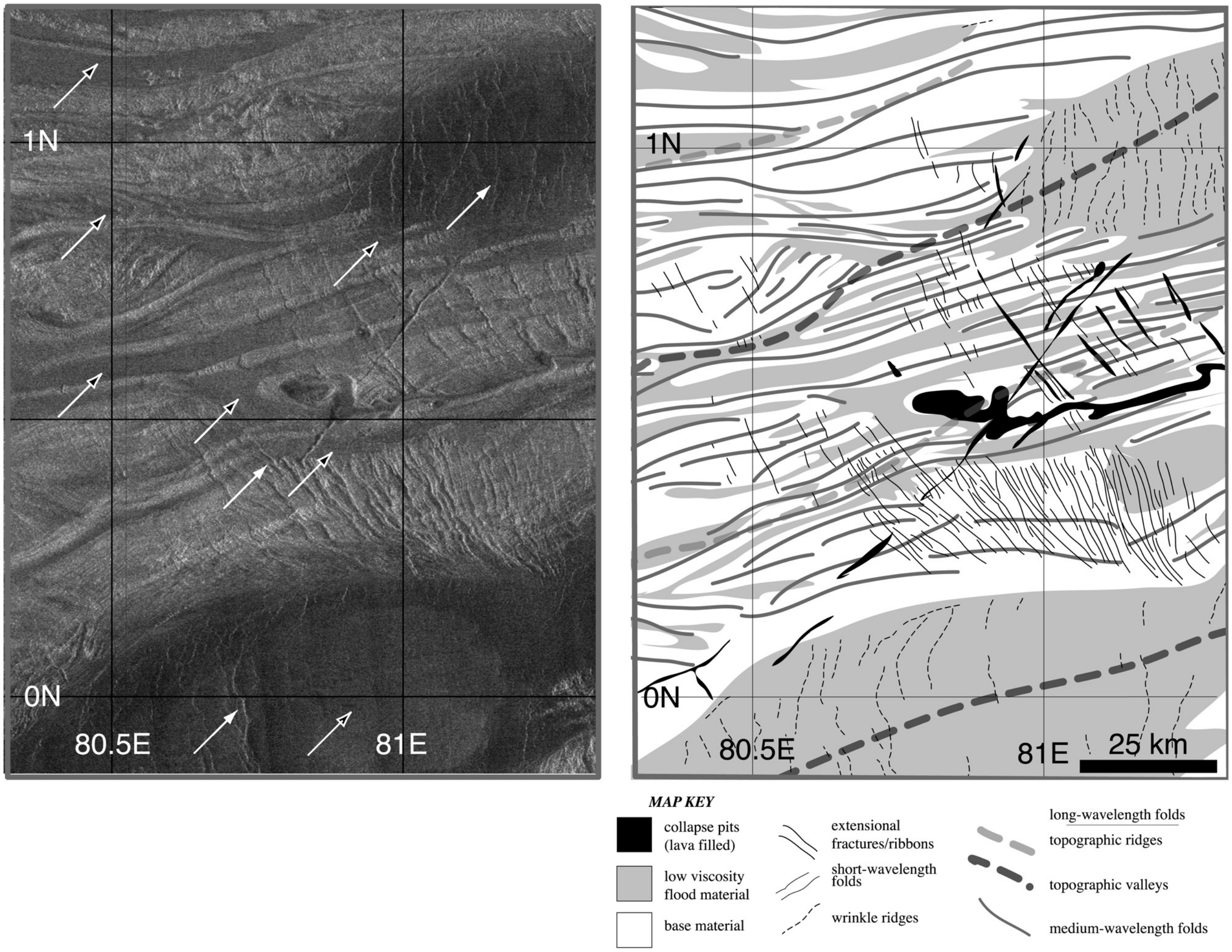

Figure 5. Left-illumination SAR image and geologic map of location B along the crest of a long-wavelength fold (see Figure. 2 for location). Note local flooding of medium-wavelength fold troughs preserved in crests, limbs and trough of long-wavelength folds. Also note late collapse pits and associated lava deposits. Black head arrows indicate flooding postdated local deformation; white head arrows indicate where deformation postdated local flooding.

material. (Because radar shadow effects could lead to the appearance of flooding, particular attention was paid to identify radar shadow effects [e.g., *Hansen et al.*, 2000]). Northwest-trending extensional structures clearly postdate the formation of the shortest wavelength folds, locally cutting fold crests and troughs, including locally flooded troughs near the center of Figure 4. In the southeast corner of Figure 4, periodically spaced ribbon fabrics that trend normal to medium-wavelength folds are locally postdated by the emplacement of low-backscatter flood material that fills local fold troughs (black arrows), yet extensional structures also cut the trough fill (white arrows) indicating that flooding locally both predated and postdated formation of various extensional structures. Elsewhere (e.g., southeast part of Figure 3), northwest-trending extensional fabrics cut fold crests and flooded fold troughs indicating that extensional strain locally postdated medium-wavelength folding and local flooding. Flooding of local lows (black arrows) is independent of local basin location with regard to long-wavelength fold crest, trough, or limb.

4.1.2. Location B

[19] Location B (Figure 5) displays flooding of medium-wavelength fold troughs (black arrows) perched along the crest of a long-wavelength fold. Again, extensional structures, which trend near orthogonal to the folds, both predate and postdate (white arrows) local flooding. Locally, short-wavelength folds trend at an angle to adjacent medium-wavelength folds. In addition, northwest-trending extensional structures parallel, and are likely reactivated as, magmatic features, although in some cases magmatic features cut at an angle to the fold crests and the extensional fabrics. The magmatic feature in the center of Figure 5 shows a central pit from which low-viscosity fluid escaped and flowed eastward, cutting a curvilinear path. Wrinkle ridges locally trend parallel to extensional structures that predated flooding of fold troughs; wrinkle ridges deform, and thus postdate, the flood material. A possible interpreted

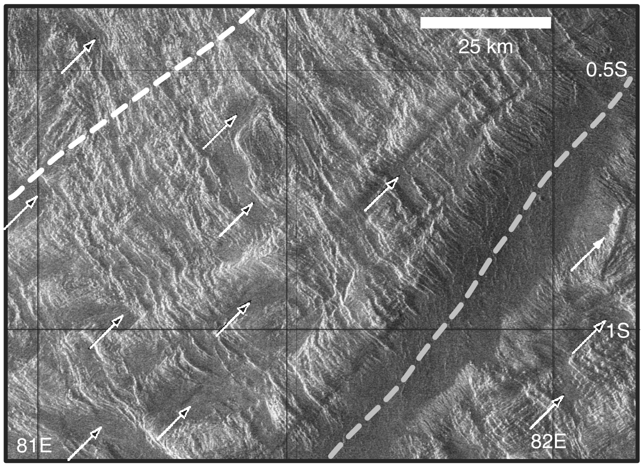

Figure 6. Left-illumination SAR image of location C across the crest (top) and trough (bottom) of long-wavelength fold (see Figure 2 for location) indicating local structural basins flooded by low-viscosity material (black head arrows). Basins are preserved along the crests, limbs, and troughs of long-wavelength folds. Flooding of short-wavelength local topographic lows located on the crest and limbs of long-wavelength folds. White head arrow marks a flood material contact that sits above the dominant flood contact. See text for discussion.

history is one of broadly synchronous layer folding and orthogonal layer extension with a progressive increase in structural wavelength with time; flooding accompanied contractional and extensional strain. I interpret that the wrinkle ridges represent inversion structures based on the interpreted history of extension, followed by flooding [e.g., *DeShon et al.*, 2000].

4.1.3. Location C

[20] Location C (Figure 6) includes a major flooded region that coincides with a long-wavelength fold trough; a fold crest trends northeastward across the top of the image. Short-wavelength folds also trend northeast; whereas short-wavelength extensional structures trend northwest. Locally, flood material fills extensional troughs located along the limbs and crests of the long-wavelength folds. Flood deposits within extensional structural lows appear isolated, indicating likely point-source flooding within different troughs. Flood material that fills the long-wavelength fold trough marks one of the youngest events across the map area, clearly postdating formation of adjacent extensional structures, and formation of the long-wavelength fold troughs. Closely spaced north-trending wrinkle ridges locally deform the trough fill. A flood material contact (white arrow) sits above the dominant flood contact, and may indicate uplift of the long-wavelength fold after initial flooding of a trough, followed by renewed trough flooding, resulting in a flood terrace. It is also possible that flood material initially flooded to a higher level along the fold trough, and then flood materials withdrew, lowering the level of flooding with time. Given the apparent asymmetry of flood terraces on the fold limbs on either side of the fold trough, the former interpretation seems more likely, although either scenario is possible.

4.1.4. Synthesis

[21] Relations from each detailed map area indicate that flooding occurred at a local spatial scale, and overlapped temporally with formation of the entirety of the tectonic fabric marked by short- to long-wavelength extensional and contractional features. At each location, shorter-wavelength fabrics predate longer-wavelength fabrics, with ductile contractional fold fabrics and orthogonal brittle extensional structures overlapping in time, hence broadly forming in a synchronous fashion. Observations of folds, extensional structures, and flooded regions across the 0N83E study area are summarized as follows. (1) Short-wavelength folds occur within the troughs, limbs, and crests of long-wavelength folds. (2) Medium-wavelength folds occur within the troughs, limbs and crests of long-wavelength folds. (3) Short-wavelength folds locally curve across longer-wavelength fold crests with angles generally <30°. (4) Low-viscosity material locally fills troughs of short-, medium- and long-wavelength folds. (5) Short- (and medium-) wavelength fold troughs show local flooding independent of location within long-wavelength folds. That is, flooded short-wavelength fold troughs occur within or along long-wavelength fold troughs, limbs and crests. (6) Locally, closely spaced extension structures cut orthogonally across short-wavelength fold crests, typically with little to no indication that these extensional structures cut longer-wavelength fold crests; these relations indicate that both layer shortening and early layer extension occurred prior to long-wavelength fold formation. (7) Ribbon structures are indeed commonly deformed by medium- to long-wavelength folds indicating relative early ribbon formation, as suggested by *Hansen and Willis* [1998]; however, ribbons also clearly cut, and therefore postdate, short-wavelength folds in many locations. Indeed, *Gilmore et al.* [1998] argued that ribbons postdated folds, although it is not clear which wavelength folds were considered. Regardless, the current analysis clearly indicates that ribbons both postdated and predated folds locally, and hence both interpretations are correct. (8) Widely spaced extension structures form complex graben, which cut folds of all wavelengths, as initially noted by *Bindschadler et al.* [1992a] and confirmed by numerous subsequent studies.

4.2. Measurements

4.2.1. Fold Wavelengths

[22] Measurement of fold suites across the field area indicates a range of structural wavelengths. Fold crests, mapped along transects normal to fold trends, were delineated using altimetry data, true stereo SAR images, and/or high contrast full-resolution SAR images. Medium-wavelength folds present the greatest challenge to wavelength determination. Table 1 summarizes structural wavelengths; measurement locations are shown in Figure 2. Determination of structural wavelength requires transects normal to structural trend that are long enough to preserve structural periodicity, and thus are uninterrupted by local flooding and/or tectonic disruption. In addition to these criteria, measurement locations were selected based on the occurrence of two or more structural elements. Areas A and D host wavelengths of short-, medium- and long-wavelength folds, and ribbon fabrics; areas B, C, E, F, and H host both contractional and extensional structures; region G hosts measurable short- and medium-folds.

[23] Area A preserves the widest range of structural elements, with wavelengths representative of the 0N83E

Table 1. Structural Wavelengths and Layer Thicknesses of Map Area 0N83E, Northern Ovda Regio, Venus

					Layer Thickness							
					Fine Folds		Medium Folds		Long Folds		Extension Fabrics	
Area	Lineament Type	Latitude	Longitude	Spacing, km	6:1, km	3:1, km	6:1, km	3:1, km	6:1, km	3:1, km	4:1, km	2:1, km
A	fine folds	−1.10	83.75	0.79	0.13	0.26						
	fine folds	−1.25	83.80	0.58	0.10	0.19						
	medium folds			2.40			0.40	0.80				
	medium folds			5.00			0.83	1.67				
	long folds			41.25					6.88	13.75		
	extension	−2.00	83.60	1.56							0.39	0.78
B	medium folds			3.45			0.58	1.15				
	extension	0.30	81.00	1.39							0.35	0.69
C	fine folds	−1.20	82.00	0.58	0.10	0.19						
	medium folds	0.75	81.25	2.08			0.35	0.69				
	extension	0.70	81.80	1.67							0.42	0.84
D	fine folds	1.75	83.75	0.71	0.12	0.24						
	fine folds	1.65	84.00	0.57	0.09	0.19						
	fine folds	1.85	84.10	0.81	0.14	0.27						
	medium folds			1.78			0.30	0.59				
	long folds			10.00					1.67	3.33		
	extension	2.25	83.85	2.17							0.54	1.09
E	fine folds	−0.60	80.15	0.71	0.12	0.24						
	extension	−0.75	80.30	1.00							0.25	0.50
F	fine folds	−0.20	81.55	0.83	0.14	0.28						
	extension	−0.25	81.75	0.88							0.22	0.44
	extension	0.00	81.75	0.74							0.19	0.37
G	fine folds	0.45	84.15	0.91	0.15	0.30						
	fine folds	0.60	84.00	0.77	0.13	0.26						
	fine folds	0.25	83.80	0.50	0.08	0.17						
	medium folds			4.50			0.75	1.50				
H	medium folds	−1.25	84.75	3.10			0.52	1.03				
	extension	−0.75	85.60	0.59							0.30	0.15
Average layer thickness					0.12 min. est.	0.24 min. est.	0.53 min. est.	1.06 min. est.	4.27 min. est.	8.54 min. est.	0.34 max. est.	0.67 max. est.

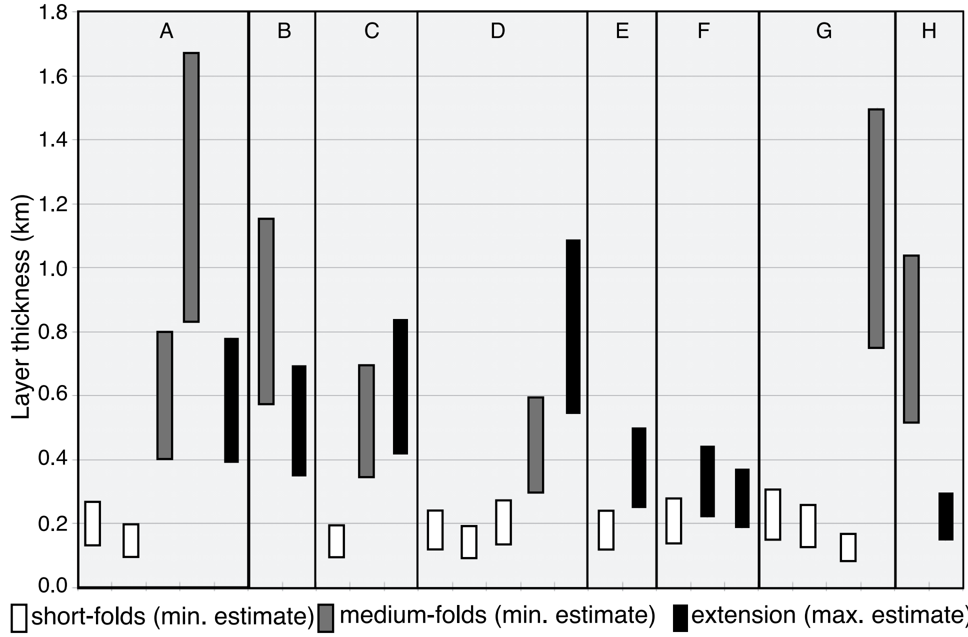

Figure 7. Plot of layer thickness associated with short- and medium-wavelength folds, and extensional structures from each of eight local study areas (data in Table 1).

study area. Ductile contractional structures (folds) range in wavelength from 0.6–0.8 km (0.7 km average) for short-wavelength folds, to 2.4–5 km (3.0 km average) for medium-wavelengths folds, to ~40-km long-wavelength folds, or warps; brittle extensional structures have wavelengths of ~0.3 to 1.6 km (1.3 km average).

4.2.2. Implications for Layer Thickness

[24] Structural periodicity reflects the presence of a rheological contrast, which could reflect a difference in layer strength or material behavior [*Montési and Zuber*, 2003]. Following previous studies [e.g., *Raitala and Black*, 1996; *Hansen and Willis*, 1996, 1998; *Ghent and Hansen*, 1999], I assume that folds within the study area formed as buckling instabilities and that extension fabrics represent brittle boudins. Empirical fold wavelength-to-layer thickness ratios of 3–6 [*Sherwin and Chapple*, 1968; *Smith*, 1977; *Huddleston and Lan*, 1995; *Kobberger and Zulauf*, 1995] constrain competent layer thicknesses during ductile folding. Field observations and analog experiments indicate that boudin wavelength-to-layer thickness ratios are generally 2–4 for brittle boudins, and as high as 10–20 for pinch-and-swell structures in which ductile flow dominates [e.g., *Talbot*, 1970; *Price and Cosgrove*, 1990; *Kobberger and Zulauf*, 1995; *Kidan and Cosgrove*, 1996]. Brittle boudin ratios are most appropriate given that extensional structures across 0N83E show dominantly brittle character. Because fabric wavelength decreases with progressive shortening strain and increases with progressive extensional strain, layer thickness estimates resulting from folds should provide minimum layer thickness estimates, whereas layer thicknesses constrained by extension fabric wavelength should provide maximum layer thickness estimates. Layer thickness estimates derived from short- and medium-wavelength folds broadly overlap the layer thickness estimates derived from extensional structures (Table 1 and Figure 7).

[25] Layer thickness estimates can be considered both on a region-to-region basis, as well as averaged across the study area. Short-wavelength folds show similar ranges in layer thickness (0.1–0.3 km) across the study area. Extension structures (excluding complex graben) show bimodal layer thickness estimates with two apparent groupings (~0.1–0.5 km and 0.35–1.1 km). These estimates of competent layer thickness generally overlap with values gleaned from ribbon terrain across 35 locations globally (0.6–2.9 km [*Ghent and Tibuleac*, 2002]). Medium-wavelength folds also show a range in layer thickness with groupings at ~0.3–0.8 km and 0.5–1.7 km. Long-wavelength folds show a range in wavelengths (and thus layer thickness estimates) from ~10 km to over 50 km. The overlap in layer thicknesses associated with short- and medium-folds, as well as extensional structures, is consistent with broad overlap in timing of these structures, as indicated independently by variable flooding of structural troughs and subsequent truncation by tectonic deformation. Relative timing of ductile and brittle structures is discussed in more detail below.

[26] Gross estimates of layer shortening can also be gleaned from fold wavelength, assuming fold formation via layer buckling. The method outlined by *Ghent and Hansen* [1999], and used herein, requires estimates of fold wavelength and amplitude, and assumes straight limbs, angular hinges, and no homogeneous layer shortening prior to fold formation. Fold wavelengths are indicated in Table 1. Fold amplitude can be estimated given Magellan SAR full resolution of 75–100 m/pixel, on the basis of the following arguments. Fold structures are observable in full-resolution SAR data; given that lineaments require three or more pixels to be identified as folds [*Stofan et al.*, 1993], fold amplitudes across the study area are likely >100 m. If folds had amplitudes smaller than 100 m they would be difficult to identify as fold structures. Taking 100 m as minimum

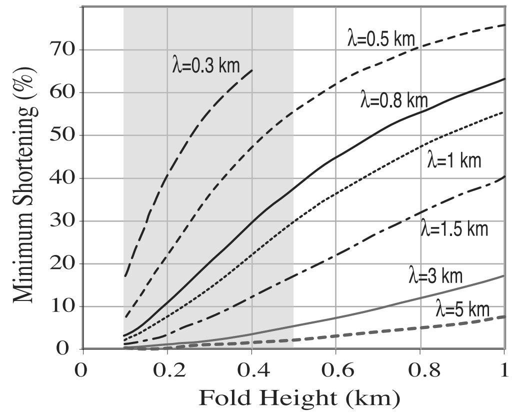

Figure 8. Plot of fold height (km) versus minimum shortening (%) for a range of fold wavelengths (λ).

amplitude for folds identified across 0N83E allows us to compare shortening estimate of various fold wavelengths. Within the resolution of the data, short-wavelength folds likely record higher values of layer shortening than long-wavelength folds. For example, short- and medium-wavelength folds have average wavelengths of 0.7 km and 3 km, respectively. These wavelengths, taken together with amplitudes of 100–150 m, result in layer shortening estimates of 3.8–8.0% and 0.2–0.5% for short- and medium-wavelength folds, respectively. By comparison, medium-wavelength folds would require amplitudes of 425–650 m to accommodate 3.8–8% layer shortening. Magellan SAR resolution places reasonable minimum limits on fold amplitudes, whereas consideration of altimetry data limits fold amplitudes as $\ll$500 m. These values, taken together with fold wavelength indicate that shorter wavelength folds likely record significantly higher values of layer shortening than longer-wavelength structures within 0N83E (Figure 8).

5. From Observation to Geologic History

[27] A cartoon block diagram (Figure 9) illustrates the salient features that must be accommodated by any proposed surface history. Long-, medium-, and short-wavelength folds show generally parallel trends across the study area, with extensional structures developed in a generally orthogonal fashion. Flood material fills local topographic lows marked by either contractional or extensional structures, and flooded regions occur within local basins independent of position across long-wavelength folds. Magmatic pit chains or troughs locally parallel extensional structures, but they also occur at angles to both extensional and contractional structures, and they locally cut even apparently young flood basins. Short-, medium-, and long-wavelength folds deform layers ranging in thickness from less than ~120–240 m, to 500–1000 m, to 4–8.5 km. Short-wavelength brittle extensional structures deform layers ranging in maximum thickness estimates of 200–1100 m. Short-, medium-, and long-wavelength folds record decreasing layer parallel shortening, with values ranging from ~8–40% for short-wavelength folds, <5% for medium-wavelength folds, and <2% for long-wavelength folds. The longest wavelength folds (>50 km) have $\ll$1% shortening [*Ghent and Hansen*, 1999].

[28] Temporal interpretations of geologic units and/or events are commonly intertwined with mechanism of emplacement or mode of deformation [e.g., *Hansen et al.*, 1999]. Given that both mechanism and temporal relations are unknown, yet the determination of each is a goal of geological mapping, internal consistency of any hypothesis remains key [*Gilbert*, 1886; *Chamberlin*, 1897]. Fundamentally, proposed temporal relations and mechanisms must be internally consistent, and they must accommodate the salient data. Therefore it is essential to consider timing and mechanism as related topics.

5.1. Fold Formation

[29] The occurrence of multiple-wavelength fold suites across the map area begs the question: how did multiple wavelength folds form? Two end-member models may be considered (Figure 10). Model A considers shortening of a rheologically layered crust with the thicknesses of individual layers corresponding to the different fold wavelengths [e.g., *Ramberg*, 1962; *Biot*, 1961; *Fletcher*, 1974; *Smith*, 1975, 1977]. Model B considers time-transgressive formation of progressively longer-wavelength folds due to layer thickness that increases with time and deformation; earlier formed short-wavelength folds are carried piggyback on later formed longer-wavelength folds due to increasing layer thickness with time. Progressive deformation of a pahoehoe lava flow surface [e.g., *Fink and Fletcher*, 1978; *Gregg et al.*, 1998] serves as a conceptual analog for model B. Each of these models makes predictions that can be compared with observations, and as such the observations serve as tests as to the viability of each model. Deformation of thin layers relative to thicker layers provides critical clues for model comparison.

[30] In the case of a rheologically layered crust (Model A) the thin surface layer should display: (1) short-wavelength

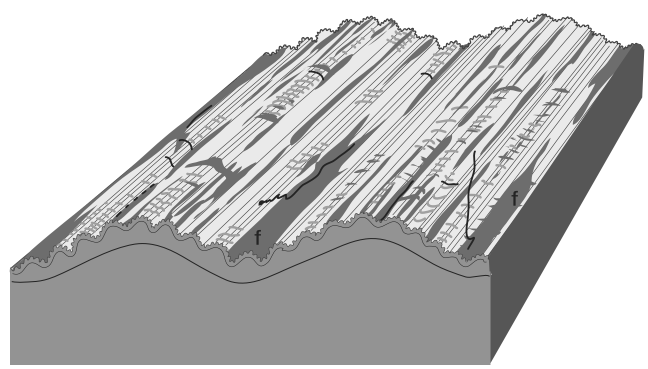

Figure 9. Cartoon block diagram that summarizes the crustal plateau structures and flooding relations observed across the study area. Relationships illustrated include: extensional structures normal to contractional structures; extensional structures cut contractional structures and visa versa; multiple fold wavelengths, independent of position on long-wavelength folds; short-wavelength folds record greater layer shortening than longer-wavelength folds; short-wavelength folds locally curve across longer-wavelength fold crests; flooding of local lows (f) independent of position on long-wavelength folds; and late pit chains (black) locally follow and cross-cut structural grain.

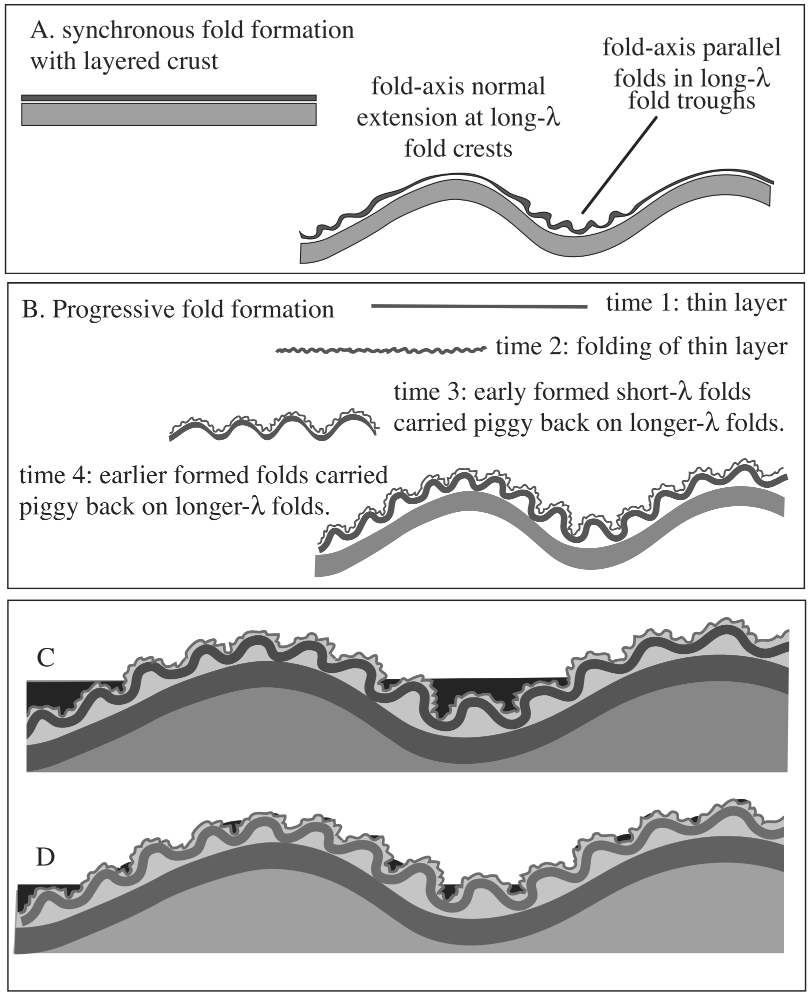

Figure 10. Cartoons of end-member models (a, b) for formation of multiple fold wavelengths and (c, d) for the relative timing of flooding and fold formation. Data relations are most consistent with progressive fold formation (Figure 10b), which results in a increase in layer thickness with increasing deformation and time (see text for more detail) and synchronous flooding and deformation (figure 10d). Figures 10c and 10d show cross-sectional views with black regions indicating flooded lows. See text for discussion.

folds within the troughs of longer-wavelength folds; (2) a lack of shortening or extensional strain along the limb of long-wavelength folds; and (3) extensional structures along longer-wavelength fold crests, with maximum extension direction perpendicular to the fold crest (Figure 10a). Predictions 2 and 3 are not met by the data. Short-wavelength folds occur across the troughs, limbs and crests of long-wavelength folds. Although extensional structures also occur within the troughs, limbs and crests of long-wavelength folds, the maximum extension direction associated with these structures is parallel to the fold crests, rather than orthogonal to the fold crest, as would be predicted. In addition, short-wavelength folds record higher shortening strain than longer-wavelength folds, which is not easily accommodated in scenario A. Thus the rheologically layered crust model does not address the data.

[31] Model B involves progressive tectonic fabric development through progressive shortening and thickening of an initially thin layer; early-formed folds are carried piggyback on later formed folds as layer thickness increases with time and progressive deformation (Figure 10b). In this case short-wavelength folds should occur equally within and along the troughs, limbs and crests of longer-wavelength folds. All folds should be collinear, although local deviations from parallel fold crests might occur. Extensional structures could form progressively during deformation. Extension structures might be expected to form orthogonal to fold axes; fold axes might be expected to form perpendicular to the direction of maximum layer shortening and extensional structures might be expected to form perpendicular to the direction of maximum layer extension. Scenario B could also accommodate the higher degrees of shortening recorded in earlier formed short-wavelength folds as compared to later formed longer-wavelength folds.

[32] Scenario B places strict requirements on the rheological structures of the evolving crustal layer. Progressive thickening of a fold layer with earlier formed folds carried piggyback on younger folds requires an exponential decrease in viscosity with depth [*Fink and Fletcher*, 1978]. If a gradational rheological contrast existed between the surface

and subsurface layers, then the surface layer would display evidence of an apparently thicker layer [e.g., *Zuber and Parmentier*, 1996]. The flooding history of the plateau surface might provide clues for the cause of the sharp decrease in viscosity with depth, as discussed below.

5.2. Flooding

[33] The timing of flooding relative to surface deformation emerges from crosscutting relations noted above, as well as the locations of flood material across the 0N83E study area. If flooding occurred late relative to surface deformation, then flood material should only fill topographic lows, and as such it should only occur in broad regions marked by long-wavelength fold troughs (Figure 10c). Although the broad long-wavelength fold troughs preserve large amounts of flood material (Figure 2), detailed relations clearly indicate that local structural troughs are flooded, including short- and medium-wavelength fold troughs, and extensional structure troughs along the crests and limbs of long-wavelength folds (Figures 3, 4, 5 and 6). Thus the observations are inconsistent with late flooding. However, if flood material leaked to the surface during progressive deformation, filling local structural lows that were subsequently carried piggyback on progressively longer wavelength structures, we would expect flooded short- and medium-fold troughs to be preserved along the crests and limbs of longer-wavelength folds (Figure 10d), as observed (Figure 9). Geologic relations indicate that flooding occurred throughout progressive deformation of the crustal plateau surface.

5.3. Synthesis

[34] Given that flooding occurred throughout the deformation history, and given that the evolution of the surface structures requires a sharp decrease in viscosity with depth, it is reasonable to propose that magma lay beneath the competent surface layer (that thickened with time and deformation). Subsurface magma could comprise the low-viscosity fluid that leaked to the surface, filled local structural lows, and crystallized to a solid, and it could also be responsible for the sharp decrease in viscosity with depth beneath the deforming surface layer. A coherent picture of the surface and near subsurface of eastern Ovda Regio begins to emerge in which the surface of the crustal plateau represents a thin competent layer over a huge pond of subsurface magma.

[35] The history that emerges requires an extremely high geothermal gradient across Ovda Regio, and by analogy, all individual crustal plateaus. This conclusion is similar to that of *Gilmore et al.* [1998] for ribbon fabric formation. (These workers argued that the high geotherm required for ribbon formation provided evidence that ribbon structures could not have formed because a plume environment could not have such a high geotherm. The results herein suggest that their initial suggestion that ribbon fabrics might require a very high geotherm to form is correct). Such a dynamic picture includes an initially thin layer ($\sim$50–100 m thick; and presumably thinner if data allowed higher-resolution observation of surface structures) that was able to deform in a ductile fashion under compression and brittle fashion under tensile stress. Given the distribution of ribbon-tessera fabric across the plateau, such a layer would have existed across the entire surface of Ovda Regio. During progressive deformation, the direction of maximum ductile shortening remained orthogonal to the direction of maximum (brittle) extension, resulting in broadly coaxial finite strain. Low-viscosity subsurface magma leaked to the surface during progressive deformation, locally flooding structural lows; once solidified, this material was carried piggyback along with earlier formed structures. The relatively strong surface layer thickened as a result of deformation and local flooding; thickening of the surface layer influenced subsequent progressive deformation, resulting in formation of longer-wavelength structures.

[36] The similarity in layer thickness estimated from short- and medium-folds and extensional ribbon fabrics is consistent with the interpretation that folds and ribbons broadly overlapped in time, as derived from crosscutting geologic relations outlined above. On the face of it one might think that contractional structures and extensional structures, and ductile and brittle structures could not form at the same time. This is possible however because materials have different strengths in compression and tension, and materials can also exhibit varying ductile or brittle behavior as a function of effective stress (e.g., tension versus compression), as well as strain rate, which can vary as a function of finite elongation. As engineers have known for quite sometime, materials commonly have different strengths in compression versus tension. Evaluating tensile strength is typically very difficult, whereas evaluating compressional strength is relatively simple. Concrete provides an example of the difference in strength of a material in compression versus tension. Because concrete is ($\sim$10 times) stronger in compression than it is in tension, builders embed steel reinforcing wires in concrete in order to increase tensile strength. Glass is also significantly stronger in compression than it is in tension. In addition, but as a separate point, the strain/deformation response of material (following elastic strain and even homogeneous thickening or thinning) can also vary under compressional stress as compared to tensile stress. Consider taffy; push it and it folds (ductile response), pull it and it can break or fracture (brittle response). The surface of pahoehoe lava flows provides a relevant geologic example; the surface of the flow can form folds (ductile response to compressional stress, formed generally normal to the flow direction) and at the same time fractures can form perpendicular to the crests of folds (brittle response to tensional stress). Thus we can envision a history for the surface across the study area in which recorded orthogonal contractional and extensional strains formed broadly at the same time.

[37] Although the generally orthogonal nature of local contractional and extensional structures across the study area indicates that the principal strain directions (X, Y, Z) remained grossly parallel to principal stress directions (σ_1, σ_2, σ_3) in a given area throughout deformation, such an assumption should be treated with great caution. Geologic relations indicate that short-wavelength structures formed before longer-wavelength structures. Therefore early-formed short-wavelength folds and orthogonal short-wavelength extensional structures would impart a mechanical anisotropy to the layer that would likely affect subsequent deformation. The short-wavelength folds, once formed, would likely greatly influence the orientation of progressively younger, longer-wavelength folds, somewhat independent of the orientation of operative principle stress directions. To clarify this

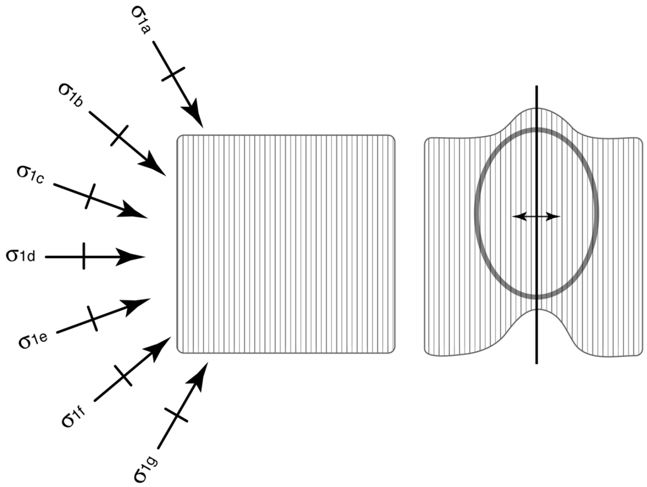

Figure 11. Corrugated cardboard experiment illustrating the finite strain ellipse (gray) that will result regardless of a wide range of possible orientations of principal compressive stress ($\sigma_{1a} - \sigma_{1g}$). Orientations of σ_1 parallel to corrugations could inhibit fold formation owing to an increase in layer strength parallel to the trend of the corrugations. Early-formed short-wavelength folds can greatly influence the orientation of younger, longer-wavelength folds (and extension structures) without requiring collinear orientation of principle stress directions throughout the deformation.

point, consider a piece of corrugated cardboard (Figure 11). A wide range of orientations of imposed maximum compressive stress directions will result in the formation of folds with axes parallel to the corrugations. Some orientations of $\sigma 1$ would actually inhibit folding owing to an increase in layer strength in a direction parallel to the trend of the corrugations. Thus early-formed short-wavelength folds can greatly influence the orientation of younger, longer-wavelength folds (and extension structures) without requiring collinear orientation of principle stress directions throughout the deformation.

6. Implications and Evaluation of Crustal Plateau Hypotheses

[38] The geologic environment and history are difficult to reconcile within the context of either the downwelling or plume hypotheses as currently stated. Downwelling requires a cold and increasing colder geothermal gradient with time, in strong contrast with the high geothermal gradient required by the data presented herein. The plume hypothesis calls for a hotter geothermal gradient than the downwelling hypothesis; however, the plume hypothesis also calls for a ductile solid subsurface, and as such, it cannot address the sharp decrease in viscosity with depth required by the data. Both hypotheses are discussed briefly in turn below.

6.1. Downwelling Hypothesis

[39] The downwelling hypothesis calls for crustal thickening by subsolidus flow and horizontal lithospheric accretion associated with mantle downwelling [*Bindschadler and Parmentier*, 1990; *Bindschadler et al.*, 1992a, 1992b; *Bindschadler*, 1995]. Previous criticisms of the downwelling hypothesis include the long time required for lower crustal flow [*Kidder and Phillips*, 1996], a predicted domical shape rather than the observed plateau shape, and a lack of documented evidence for crustal shortening [e.g., *Hansen et al.*, 1999, 2000]. The previous studies did not, however, consider potential shortening recorded by short- and medium-wavelength folds. As shown herein these structures could record minimum layer shortening up to 50%, and as such, might be interpreted as support for the downwelling hypothesis. Despite this, there are several factors that cannot be addressed within the context of the downwelling hypothesis. The downwelling hypothesis predicts an initially cool and progressively colder geothermal gradient during crustal plateau formation. A cool or even cold gradient was predicted as a driver for the negative buoyancy that leads to crustal thickening due in a mantle sinker. However, the results presented herein indicate that the crustal plateau environment was marked by an extremely hot, rather than cold, geothermal gradient, with magma existing at shallow depth beneath the entire crustal plateau surface during much of the surface deformation. In addition, the downwelling hypothesis cannot accommodate: (1) surface extension throughout deformation, as previously noted; (2) orthogonal shortening and extension throughout tectonic evolution of the plateau; (3) the extremely thin layer thickness during earliest deformation; (4) differential shortening of thin and thick layers, rather than shortening of a rheologically layered crust as predicted; (5) an exponential decrease in viscosity with depth with a solid layer above a liquid; and (6) widespread emplacement of flood material, presumably lava, throughout the deformation history. Perhaps most important, several observations taken in concert indicate an extremely high geothermal gradient, counter to that predicted for a downwelling scenario. Thus the downwelling hypothesis is not viable.

6.2. Plume Hypothesis

[40] Although the plume hypothesis calls for a significantly higher geothermal gradient than in a downwelling case, it also cannot account for all of the observations delineated herein, as well as salient features of the surface history. As noted by *Gilmore et al.* [1998], the thermal environment required by crustal plateau structures is inconsistent with that associate with a mantle plume. The plume hypothesis [*Hansen et al.*, 1997; *Hansen and Willis*, 1998; *Phillips and Hansen*, 1998; *Hansen et al.*, 1999, 2000], calls for ductile flow of the crust resulting in destruction of all previous structural features, including impact craters and earlier formed structures, prior to formation of delicate ribbon (and fold) structures. According to the hypothesis, cooling of the ductile crust led to the development of a thin competent surface layer, which recorded the progressive deformation that accompanied crustal plateau evolution. A key problem is that the plume hypothesis calls for ductile (i.e., plastic but solid) material beneath this competent surface layer. A ductile solid beneath the competent surface layer will not, however, allow for the formation of short-wavelength folds, or the progressive formation of short-, medium-, and long-wavelength folds. This problem is elegantly highlighted through robust finite-element modeling specifically designed to address the formation of short-wavelength folds [*Ghent et al.*, 2005]. Modeling results indicate that if a ductile, but solid, subsurface material is hot enough to provide a sharp decollement, the competent

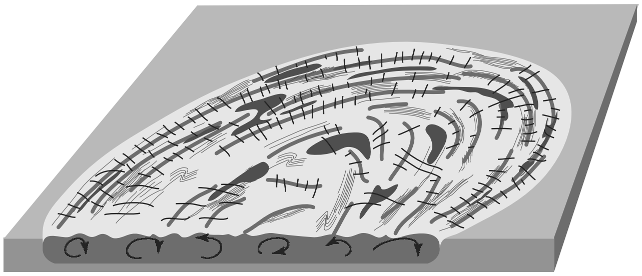

Figure 12. Cartoon illustrating the formation of ribbon tessera terrain.

surface layer cannot develop significant structural topography, as required by crustal plateau observations. However, a cooler environment, which might allow surface structural topography to develop, results in the formation of folds with wavelengths much longer than the short-wavelength folds developed across the study area. The results here indicate that the rheological structure of the plateau environment during surface deformation is that of an exponential decrease in viscosity with depth with a solid layer above a liquid.

[41] Thus a principal problem with the plume hypothesis lies, critically, with the nature of the subsurface material, that is, the material underlying the thin competent surface layer. Although a sharp decollement between the competent surface layer and the subsurface material is required, perhaps more important, is that a very sharp, exponential, decrease in viscosity is also required. This viscosity gradient is so sharp as to require a downward phase change from solid to liquid [*Fink and Fletcher*, 1978]. This requirement for a deeper melt layer was not previously recognized, and is not accommodated within the context of the plume hypothesis as published. The required exponential decrease in viscosity with depth indicating the presence of a liquid beneath the solid surface layer, together with a required subsurface source of flood material regionally across the plateau can be accommodated within the context of a subsurface magma across the plateau. This suggests that subsurface material was liquid, not a ductile solid, as proposed within the plume hypothesis, and as such requires a completely different crustal environment than that proposed by the plume hypothesis. It is reasonable to conclude that the subsurface material was magma, and this realization leads to the proposal of an entirely new hypothesis for crustal plateau formation, the lava-pond hypothesis.

7. Lava Pond Hypothesis

[42] The lava-pond hypothesis calls for progressive solidification and deformation of the surface of a large lava pond with an areal extent similar to that of an individual crustal plateau. Ribbon-tessera terrain represents lava pond ‘‘scum,’’ a competent surface layer that congeals across the lava pond (Figure 12). Folds form by selective amplification of instabilities in the congealed surface as a result of layer shortening, likely driven by convection in the magma. Extensional fabrics (ribbons) form normal to the fold crest, tracking maximum principal extension. Subsurface magma variably leaks to the surface as lava, flooding local lows in structural topography and solidifying. With time the surface layer thickens as a result of deformation (principally contractional deformation resulting in layer thickening), cooling and resulting growth of the solid layer as the solidus isotherm, and hence the solid-liquid boundary, migrates downward, leading to layer thickening. Layer thickening also results from local flooding and subsequent solidification of lava within structural lows. As the surface layer (pond scum) thickens, longer wavelength contractional (folds) and extensional structures (ribbons) form. The respective parallelism of longer-wavelength fold and extensional structures with shorter-wavelength folds and ribbons likely results from the fabric anisotropy inherited from immediately preceding deformation. One might interpret a parallelism of principal stress directions through time and deformation, due to the apparent coaxial nature of interpreted incremental principal strain axes. However, once a fabric anisotropy is developed it can be reinforced and enhanced, just as shortening of a corrugated layer results in parallelism of longer-wavelength folds despite a wide range of possible principal stress directions. The collinear nature of contractional structures and perpendicular, but also mutually collinear, extensional structures, therefore probably does not track principle stress directions through time. Instead these track the principle strain orientations.

[43] Venus’ supercritical atmosphere of dense carbon dioxide may have played a key role in the nature of the pond scum solidification, presumably allowing it to remain ductile over a significant period of time, in strong contrast to the cooling of a lava lake surfaces on Earth; Venus’ atmosphere acts more like a conducting layer than a convection layer with regard to heat transport, and as a result lava cools more slowly than on Earth [*Snyder*, 2002]. The rheological environment that would result should be robustly investigated with specific attention to the development of pond scum fabrics. Such a study is, however, outside the scope of the current contribution.

[44] Other published studies aimed at understanding the surface history of various parts of Ovda Regio might also be interpreted within the context of the lava-pond hypothesis. Early study of tessera terrain fabrics led to the identification of so-called ‘‘lava-flow-terrain-tessera’’ [*Hansen and Willis*, 1996]. This distinctive tectonic fabric, only recognized within Ovda Regio to date, is illustrated in Figure 13. The fabric is comprised of extremely short-wavelength marked locally by folds, ribbons, and in some cases, lineaments that cannot be robustly identified as either extensional or contractional. Ribbons and folds appear to be deformed into chevron-like folds, with the resulting fabric appearing similar to that of a piece of rumpled corduroy. Wavelengths within the lava-flow-terrain-tessera are at the resolution of ridges in Magellan SAR data, yielding values of <0.3 km. This terrain originally was named based on its characteristic similarity to the surface of pahoehoe lava flows, though of a vastly different scale [*Hansen and Willis*, 1996]. Another example includes ribbon structures, which require that the crustal plateau surface was healed of all previous structures prior to ribbon structure formation [*Hansen and Willis*, 1998]; This requirement can be accommodated within the context of the lava pond hypothesis because the surface layer would have crystallized directly from a magma, and therefore it would not record a complex fracture history, as is typical across much of Venus’ surface [e.g., *Banerdt et al.*, 1997].

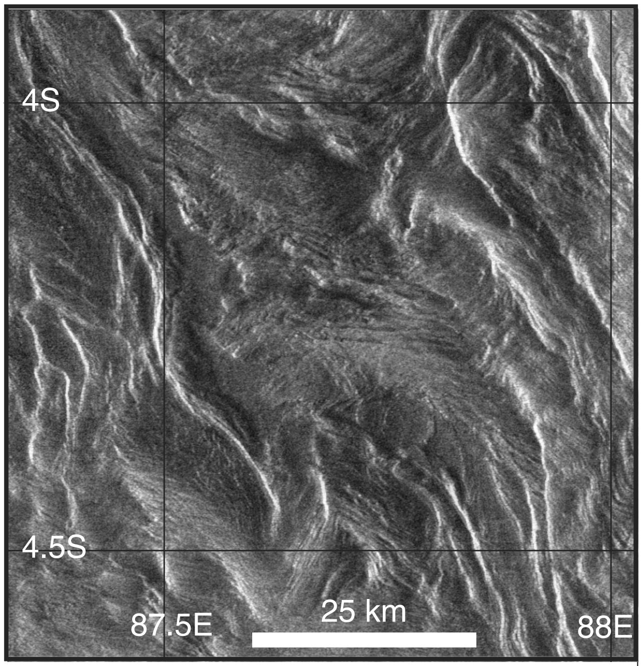

Figure 13. Left-illumination SAR image of "lava-flow tessera terrain" with chevron folds, Ovda Regio [see *Hansen and Willis*, 1996]. Note lineaments to scale of effective resolution (~0.3 km spacing) involved in chevron-like folds.

[45] Other workers have also recognized the ductile character of Ovda Regio's tectonic fabric, or ribbon-tessera terrain. Recent studies highlight the occurrence of ductile shear zones within various parts of Ovda Regio, including along the southern margin, central Ovda [*Romeo et al.*, 2005; *Ignacio et al.*, 2005], and along the eastern boundary of Ovda Regio with Thetis Regio to the east [*Ghail*, 2002; *Tuckwell and Ghail*, 2003; *Kumar*, 2005]. These shear zones display variable ductile and brittle structures that together describe coherent pictures of noncoaxial shear, similar to S-C fabrics within terrestrial ductile shear zones. These zones could represent shear zones formed within the surface of the crystallizing lava pond. Hawaii's lava lakes show dynamic flow fabrics of extension, convergence and strike-slip translation similar to terrestrial plate tectonic kinematic patterns, presumably driven by convection within the lava lake. Similarly Ovda's ancient lava pond surface could record layer-parallel shortening and orthogonal extension, along with localized strike-slip shear distributed over several hundreds of kilometers. *Hansen* [1992] first described noncoaxial fabrics within tessera terrain fabrics of Itzpapalotl Tessera in Venus' Ishtar Terra. This broad (~300 km wide) sinistral shear zone forms the boundary of high-standing tessera terrain with adjacent lowland to the north. Many zones of so called "S-C tessera terrain," which record ductile noncoaxial strain fabrics [*Hansen and Willis*, 1996], occur along the boundary of crustal plateaus, or along the boundary of large arcuate inliers and adjacent lowland, which would be consistent with the boundary-related shear formed along lava pond "shorelines" or margins.

[46] In some cases, the occurrence of S-C tessera terrain fabric has been interpreted as related to plate scale "indenters" and collision tectonics, and thus put forth as evidence of plate tectonic processes on Venus [e.g., *Tuckwell and Ghail*, 2003; *Romeo et al.*, 2005]. This interpretation seems flawed, however, because (1) there is no apparent crustal indenter, as in the case of India with the Asian plate on Earth [e.g., *Tapponnier et al.*, 1982], and (2) the morphology of S-C tessera terrain records surface deformation structures. That is S-C tessera terrain fabrics do not represent eroded deeper-level crust where material can flow in a ductile fashion, as is the case for terrestrial shear zones. The brittle-ductile character of S-C tessera terrain, while noncoaxial in nature, is not directly correlative with terrestrial shear zones because the latter form at depth and are subsequently exposed owing to extensive erosion and removal of overlying material. Comparison with a terrestrial shear zones would yield few similarities with S-C tessera terrain because erosive processes highlight quite different aspects of a rock than the geomorphologic expression that results from topographic expression of structural features, as is the case of S-C tessera terrain. Venus' S-C tessera terrain, which records deformation at the surface, exhibits a ductile character as noted by many workers [*Hansen*, 1992; *Hansen and Willis*, 1996; *Tuckwell and Ghail*, 2003; *Kumar*, 2005; *Romeo et al.*, 2005]. The entire crustal plateau surface displays a ductile character of deformation fabrics, as well as kinematically coherent brittle deformation, indicating that the surface deformed simultaneously in both brittle and ductile modes. Rocks can deform in this fashion at midcrustal levels on Earth, but they do not deform in this manner on the surface of the Earth. In general, away from crustal plateaus, rocks at Venus' surface deform quite similarly to rock at Earth's surface. Despite the much higher surface temperature on Venus, which might allow rocks to deform through ductile processes such as viscous creep, Venusian rocks are quite strong as a result of their extremely dry state [*Mackwell et al.*, 1998]. However, the nature of the deformation fabric is unique within Venusian crustal plateaus, and arcuate inliers of ribbon-tessera terrain in Venus' lowland. What makes these regions unique is the uniformly ductile character of their deformation patterns. The very fact that we can recognize coherent tectonic patterns over huge areas provides a clue to the surface evolution. This continuity in structural pattern results from ductile deformation and indicates that over these huge areas, covering several millions of square kilometers, Venus' surface deformed in a ductile fashion. Although tessera terrain fabrics show a range of characteristic fabrics, each of these fabrics shares evidence of ductility [see *Hansen and Willis*, 1996, Figure 3], with the exception of tessera terrain of Phoebe Regio. I propose that this ductility reflects the extremely hot environment of crustal plateau tessera terrain formation in the past, resulting from progressive deformation and solidification of huge lava ponds representing individual crustal plateaus.

8. Formation of Huge Lava Ponds

[47] How could such a large volume of lava form concurrently over an area the size of an individual crustal plateau? Crustal plateaus lack evidence of massive volcanic structures, and, paradoxically, even the largest terrestrial

volcanoes are dwarfed by comparison to Venus' crustal plateaus. Although not representative of a single volcanic construct, the greater Ontong Java plateau, one of Earth's large igneous provinces (LIPs), covers an area similar to that of individual crustal plateaus on Venus. The Ontong Java plateau has been proposed by many to be the surface signature of a deep mantle plume [e.g., *Tarduno et al.*, 1991; *Bercovici and Mahoney*, 1994; *Coffin and Eldholm*, 1994; *Farnetani and Richards*, 1994; *Farnetani et al.*, 1996; *Ito and Clift*, 1998; *Ito and Taira*, 2000]. However, as noted above, a mantle plume mode of formation is not likely for Venusian crustal plateaus. Recently, however, *Ingle and Coffin* [2004] proposed that the submarine Ontong Java plateau, which rises 2–3 km above the surrounding ocean floor, may have formed as the result of massive partial melting of the mantle caused by the impact of a large bolide on relatively young (and hence thin) oceanic lithosphere, following earlier suggestions [*Rogers*, 1982; *Price*, 2001]. In a similar vein, *Reese et al.* [2004] proposed that the Tharsis volcanic region of Mars might have formed as the result of a bolide impact.

[48] Despite contrary arguments by *Ivanov and Melosh* [2003], there is growing support for the notion that large bolide impacts can result in the formation of large melt volumes. Critical factors that contribute to melt formation include: (1) lithospheric thickness, with thinner lithosphere favoring melt production; (2) potential temperature of the mantle, with a 50 °C change in temperature leading to increased melt volumes by 2–3 times; (3) bolide size (or, impact crater diameter): the larger the bolide (crater) the larger the total melt volume; (4) bolide velocity; and (5) assumptions regarding melt formation, and perhaps more importantly, melt crystallization [see *Jones et al.*, 2005; *Elkins-Tanton and Hager*, 2005]. Modeling by *Jones et al.* [2005] and *Elkins-Tanton and Hager* [2005] indicates that an impact event creating an impact crater on the order of 200–300 km diameter (20- to 30-km bolide) on 30- to 50-km-thick lithosphere with a mantle potential temperature of 1350°C could generate melt volumes on the order of $2–7 \times 10^6$ km^3. Such a volume (or even smaller volumes) could easily account for the volume of an individual Venusian lava pond, as postulated here. Building on the bolide-melt ideas, I propose here that lava pond magma formed due to massive partial melting of Venus' mantle caused by the impact of a large bolide on ancient thin Venusian lithosphere.

[49] Although models cited above were constructed for bolide impacts on Earth, the critical parameters are applicable to ancient Venus. In fact, ancient Venus might be even better suited to impact melt generation than Earth. It is widely accepted that ancient Venus had a globally thin lithosphere [e.g., *Solomon*, 1993; *Grimm*, 1994b; *Solomatov and Moresi*, 1996; *Schubert et al.*, 1997; *Phillips and Hansen*, 1998; *Brown and Grimm*, 1999], one of the most critical factors of impact melt generation [*Jones et al.*, 2005]. The potential temperature of Venus' mantle is generally taken as similar to Earth's, and like Earth, was likely hotter in the past. As discussed in detail by *Jones et al.* [2005], total melt volumes depend critically on melt crystallization, a process that is likely inhibited by Venus' dense atmosphere of supercritical CO_2 [*Snyder*, 2002]. That is, total melt volume (the volume of melt that exists at a particular time) depends on the amount of melt that forms, but also on the volume of melt that remains as melt. Flash freezing, which would lead to lower total melt volumes [e.g., *Ivanov and Melosh*, 2003], should be minimized in the Venus environment. Furthermore, Venus' supercritical CO_2-rich atmosphere, which acts more like a conductive medium than a convective medium in terms of heat transfer [*Snyder*, 2002], would further inhibit lava crystallization at time-scales well beyond a catastrophic impact event, and as such allow large total volumes of lava to persist over time. Taken together, all of these factors, combined with current ideas of Venus' ancient environmental conditions, suggest that large-volume impact-generated melting should be considered a viable process for ancient Venus.

[50] Large bolides (20–30 km diameter) were also more common in early solar system history, and thus in Venus' past. It is not entirely clear how large a bolide would need to be. The required size of an effective bolide is intrinsically tied to several factors, each of which is strictly unknown, including ancient lithosphere thickness, bolide composition, and melt-impact processes, presumably the presence of large bolides would not be a major challenge to the lava pond hypothesis. Mead Crater, Venus' largest impact crater, at ~270 km diameter provides evidence of a bolide-impact of the postulated size (~27 km diameter) in Venus' more recent past. In the case of Mead Crater, massive melting did not occur, presumably because the lithosphere was thick at the time of impact. Thus a most critical parameter for impact-induced melting, thin lithosphere, was not met during the formation of Mead Crater, despite the presence of a large bolide impact.

[51] Assuming that bolide-induced melting could occur on ancient Venus, we can consider the geological consequences (Figure 14). Beginning with a globally thin lithosphere, impact of a bolide large enough to form a 200- to 300-km-diameter crater would cause massive partial melting in the upper mantle. The melt would rise buoyantly to the surface where it could collect, forming a huge lava pond, significantly larger than the crater diameter. Melt should rise quickly to the surface given the fractured nature of the crust, and the lower density of the melt. The collection and rise of partial melt in Earth's mantle is an extremely complex problem, as evidence by many terrestrial studies event [e.g., *Choblet and Parmentier*, 2001; *Braun et al.*, 2000; *Jha et al.*, 1994], even outside the context of an impact. These topics are beyond the scope of the current contribution and an exciting area for future work. Clearly there are a number of factors that are currently outside the limits of known, or well-accepted geological processes as we postulate large impact events on Venus. I submit however, that the melt will rise to the surface, likely through fracture systems resulting from the impact following suggestion of *Jones et al.* [2005]. As indicated by *Jones et al.* [2002, 2005], the initial impact crater would be auto-obliterated. We might also expect the impact event to have an effect on regional topography, including an area significantly larger than the crater itself. The nature of the effect would depend on the size and composition of the bolide, as well as the thickness and rheology of Venus' lithosphere at the time of impact. The regional extent of any particular lava pond would presumably reflect local to regional topographic features, including the regional effects of the impact event. The impact event might well cause the formation of a regional-

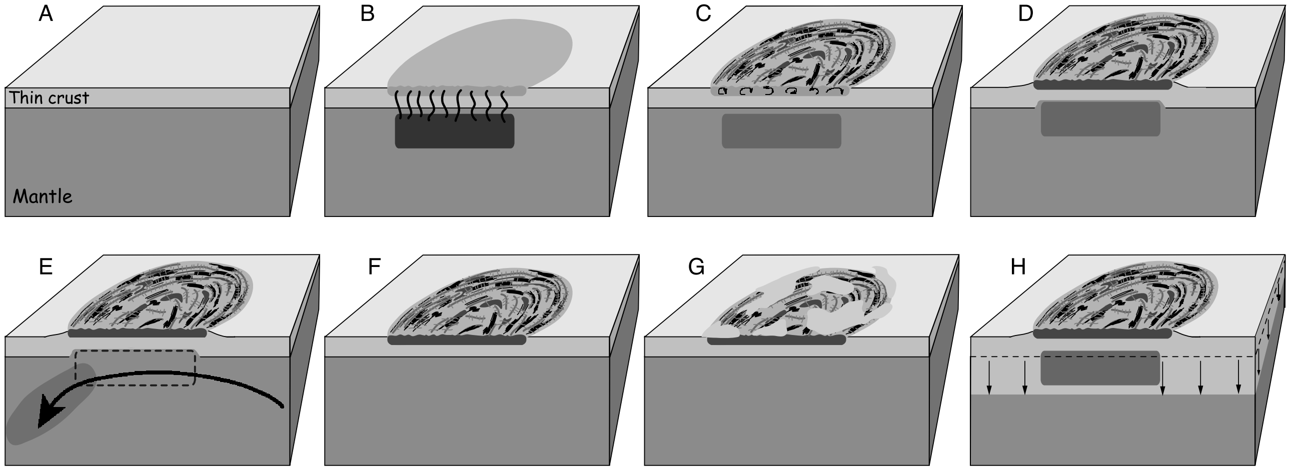

Figure 14. Cartoon sequence of block diagrams illustrating crustal plateau formation and collapse following the lava pond via bolide impact hypothesis and an indication of how plateaus could be preserved, escaping collapse. (a) Block showing mantle and thin crust, a global condition of ancient Venus. (b) Massive partial melting occurs in the shallow mantle (dark gray), induced by a bolide impact; the melt rises buoyantly (black wavy lines) to the surface forming a huge lava pond. (c) Convection in the lava pond results in surface deformation, and local leaking of lava to topographic lows resulting in the formation of the distinctive tessera terrain tectonic fabric that characterizes crustal plateaus. In the mantle, the region that experienced massive partial melting forms a lens of low-density residuum (dark gray). (d) Isostatic adjustment resulting from the low-density residuum results in surface uplift of solidified (or nearly solidified?) lava pond, and formation of the crustal plateau feature. During plateau uplift long wavelength warps (50–100 km) form (not shown) as a result of E-V-P rheology or rheologically layered crust (see text). Crustal plateau formation is complete. (e) Mantle convection at any time after plateau formation could strip away the low-density residuum root, resulting in (f) subsidence, or ultimate collapse of the plateau. (g) Emplacement of thin localized deposits cover distinctive tessera-terrain fabric locally, but the exposed regions preserve a record of the ancient lava pond surface. (h) Crustal plateaus could be preserved as highland regions as a result of lithosphere thickening (presumably the result of secular cooling and a global transition to thick lithosphere (see text)) locking in the low-density residuum root, and thus preserving the high-standing plateau decorated by lava pond deformation fabrics (ribbon tessera terrain).

scale topographic basin, which could influence the general shape and boundaries of the genetically related lava pond. Additionally, a region much larger than the initial impact would be completely "resurfaced," flooded by eruption of lava pond magma. The lava pond itself would solidify over time and pond "scum" would form the distinctive and characteristic ribbon-tessera terrain. At depth within the mantle, the region from which partial melt was extracted would leave behind a large lens of depleted solid residuum. The lens of melt residuum would be compositionally more buoyant (lower density) and stronger (higher melting T) than the undepleted adjacent mantle [*Jordan*, 1975, 1981]. Isostatic adjustment due to the lower density residuum lens would result in surface uplift, elevating the solidified (or solidifying) lava pond above the surrounding lowland region. During uplift, long-wavelength warps (50–100 km) would form as a result of differential uplift of rheologically layered crust. With isostatic uplift driven by the low-density residuum root, the solid lava pond massif would form an uplifted crustal plateau. However, the evolution need not end here. Because the crustal plateau root resides in the ductile mantle rather than in the lithosphere (as previously assumed within the context of the downwelling and plume hypotheses), the residuum root could be stripped way by mantle convective processes. If residuum were stripped away, either partially or completely, the overlying crustal plateau would subside in accordance with the amount of displaced (removed) residuum. An individual crustal plateau might subside to the level of the adjacent lowland, or to an intermediate level. If, however, secular cooling led to lithospheric thickening prior to removal of the residuum root, then the residuum root would become "frozen" in place, and the overlying crustal plateau would be preserved as a high-standing feature. By this proposed mechanism, crustal plateaus could preserve a range of elevations from high-standing Ovda Regio to subsided inliers of ribbon tessera preserved across many lowland regions. The ribbon-tessera terrain inliers would preserve remnants of ancient lava ponds, and a record of ancient large bolide impact events. Thin surface deposits could partially or completely cover the distinctive ribbon-tessera (pond scum) fabrics, obscuring or erasing, respectively, evidence of ancient lava ponds. Thus the lava-pond bolide impact hypothesis could account for the wide range of topographic expression of crustal plateaus, as well as "collapsed crustal plateaus" of Venus' lowland.

[52] Although there is a relatively strong spatial correlation of tessera terrain fabric with crustal plateau topography [e.g., *Bindschadler et al.*, 1992b; *Phillips and Hansen*, 1994, 1998; *Hansen et al.*, 1997; *Ghent and Hansen*,

1999], detailed mapping indicates that in some places coherent tessera fabrics extend into adjacent lowlands, as is the case of Tellus and Ovda regions [e.g., *Senske*, 1999; *Hansen*, 2006a]. In the context of the proposed hypothesis, the lava pond, responsible for ribbon terrain fabric, forms on the surface, whereas the residuum, responsible for elevation, forms at depth in the shallow ductile mantle. Although we might expect broad correlation of surface and subsurface features, one can also envision situations in which the correlation would not be exact, and lava pond scum, or ribbon-tessera terrain, could be variably uplifted owing to mismatch of surface lava pond and subsurface residuum. It is important to understand that the timeframe of lava pond formation and solidification would differ from isostatic adjustment owing to mantle melt-residuum (the plateau-uplift event), similar to the time lag of isostatic rebound and the disappearance of continental ice sheets. Thus a lava pond would form at the surface, solidify, and be uplifted later, and at a very different rate than lava pond solidification.

[53] In another vein, there is growing evidence that shield terrain, marked by extensive small (1–10 km diameter) shields and an associated veneer of coalesced volcanic shield deposits [*Hansen*, 2005a], might be spatially correlative with ribbon-tessera terrain [e.g., *Aubele*, 1996; *Hansen*, 2005a, 2006a; *Lang and Hansen*, 2005]. Although testing this postulated relationship requires further detailed geologic mapping, such a correlation would be compatible with the lava pond-impact hypothesis. If, as postulated herein, lava pond magma results from massive partial melting of the mantle, the melt would be enriched in radiogenic elements; thus ribbon-tessera terrain, which represents solidified pond scum, might also be enriched in incompatible radiogenic components. This enrichment in radiogenic material could in turn contribute to subsequent local in situ partial melting to form volcanic shield terrain [e.g., *Hansen and Bleamaster*, 2002; *Hansen*, 2005a]. Thus point source melting might occur in crust that evolved directly by prior, bolide-induced, massive partial melting of the mantle.

[54] Finally, lava-pond via bolide-impact formation of crustal plateaus could provide a mechanism for large-scale ($2–5 \times 10^6$ km^2) but "local" resurfacing that is below the detectable spatial limit of crater statistics [*McKinnon et al.*, 1997; *Campbell*, 1999]. Preexisting craters would either be completely destroyed, or preserved, depending on their proximity to the impact site. Specifically, preexisting craters would be essentially obliterated across the entire region of the soon-to-form crustal plateau, effectively resetting the local surface age across individual plateaus to "zero" at the time of bolide impact. This would allow for complete resurfacing at a large scale in particular areas, allowing for equilibrium resurfacing across Venus, but without the expectation of partially buried impact craters [*Hansen and Young*, 2006; *Hansen*, 2005b].

[55] *Hamilton* [2005] proposed that Venus' crustal plateaus represent the results of large bolide impact on Venus' surface. However, in the work of *Hamilton* [2005], the model, presented in a few short sentences, is not well developed, and it does not address several factors including: (1) the elevated character of crustal plateaus; (2) the formation of individual structural patterns across plateaus; and (3) the formation of collapsed crustal plateaus preserved within Venus' lowland regions. In addition, *Hamilton* [2005] postulated that the radar-smooth material collected in the long-wavelength fold troughs represents sediment, presumably eroded from high reaches within the plateau. Thus, within the context of the *Hamilton* [2005] hypothesis, the observed tectonic structures (ribbon-tessera terrain ribbons, folds, and graben) should represent eroded surfaces, rather than the primary morphology of tectonic structures. These views are not supported by the current study. *Hamilton* [2005] also inferred that the ancient lithosphere of Venus was quite thick, yet the impact of a large bolide on thick lithosphere would not induce the formation of large volumes of partial melt [e.g., *Ivanov and Melosh*, 2003; *Jones et al.*, 2002, 2005; *Elkins-Tanton and Hager*, 2005]. The bolide-induced lava-pond hypothesis for crustal plateau formation outlined herein has little resemblance to the hypothesis of *Hamilton* [2005].

[56] As noted by *Jones et al.* [2005], bolide impact might lead to the generation of huge melt volumes, but it could also spawn a moderately shallow mantle plume that could affect crustal plateau formation. Some might argue that a mantle plume could also cause the amount of melting required here, without an impact event. The amount of melting that can be generated by a mantle plume is hotly debated, but in any case, such a model would differ from published versions of the plume hypothesis for crustal plateau formation, as cited herein. The arrival of a hot, buoyant, ascending mantle plume might generate large volumes of melt at the surface, as a result of voluminous decompression melting, and a combination of thermal expansion, buoyant uplift [e.g., *Farnetani and Richards*, 1994; *Griffiths et al.*, 1989; *Ito and Clift*, 1998]. In the case of a mantle plume, however, the relative timing of lithospheric uplift and melt migration to the surface might be quite different than predicted for the evolution of crustal plateaus. Lithospheric uplift, driven by thermal expansion, could reach or exceed 4 km, but it would predate or accompany thinning of the lithosphere, and it should predate delivery of melt to the surface, given that partial melting is caused by decompression [*Farnetani and Richards*, 1994; *Griffiths et al.*, 1998]. Therefore the lava, once at the surface, might be expected to flow regionally outward from a regional plume-head generated topographic gradient, rather than collect and form a regional-scale lava pond. In contrast, in the case of a large-bolide impact event, a regional-scale basin might be expected to form, which could serve to collect melt as it leaked to the surface, presumably through extensive lithospheric fractures caused by the impact event. Clearly a revised plume model should be investigated in future work, but the bolide-impact hypothesis currently seems most promising to the author.

[57] There are many aspects of the lava-pond hypothesis and the bolide-impact hypothesis that might be tested with future work including, but not limited to: mode, and amount of melt generation as a result of bolide impact; transfer of melt to the surface; the effect of bolide impact on regional-scale topography; details of lava pond solidification in a Venus atmosphere; detailed structural mapping of Venus' other crustal plateaus in order to test the geologic history of plateau surfaces as proposed herein; detailed geologic mapping of lowland regions in order to determine whether "rootless" lava ponds could have existed, or not; modeling aimed at testing the viability a melt-residuum root; and

modeling aimed at testing if a residuum root could be swept away through subsequent mantle convection processes. At this nascent stage in our understanding of Venus tectonics, it seems reasonable to consider the lava-pond bolide impact hypothesis for crustal plateau formation. At the very least, consideration of such a different hypothesis could lead to further refinement of many parameters of crustal plateau evolution and Venus surface evolution [*Chamberlin*, 1897; *Gilbert*, 1886].

9. Summary

[58] Detailed geologic mapping of a 6° by 6° region of eastern Ovda Regio provides new clues for the formation of Venusian crustal plateaus. Long-, medium-, and short-wavelength folds show generally parallel trends across the study area, with extensional structures developed in a generally orthogonal fashion. Flood material fills local topographic lows marked by either contractional or extensional structures, and flooded regions occur within local basins independent of position across long-wavelength folds. Magmatic pit chains or troughs locally parallel extensional structures, but they also occur at angles to both extensional and contractional structures, and they locally cut even apparently young flood basins. Short-, medium-, and long-wavelength folds record decreasing layer parallel shortening, and increasing layer thickness. Layer thickness derived from short-wavelength folds (0.1–0.3 km) and extension structures (showing bimodal layer thickness of ~0.1–0.5 km and 0.35–1.1 km) generally overlap with one another and with values gleaned from global exposures of ribbon terrain (0.6–2.9 km). Medium-wavelength folds indicate an increase in layer thickness (~0.3–0.8 km and 0.5–1.7 km). Long-wavelength folds (~10 km to over 50 km) correspond with layer thickness >6 km. The overlap in layer thicknesses associated with short- and medium-folds, as well as extensional structures, is consistent with broad overlap in timing of these structures if the subsurface material is molten. This relationship is corroborated by flooding relations, which indicate that local flooding accompanied progressive layer deformation.

[59] Documented relations are consistent with a surface evolution that involves progressive shortening and thickening of an initially thin layer; early-formed folds were carried piggyback on later formed folds as layer thickness increased with time and progressive deformation. Extension structures developed orthogonal to fold axes. This history places strict requirements on the rheological structures of the evolving crustal layer, requiring an exponential decrease in viscosity with depth with a transition from solid to liquid. These relations are consistent with a postulated subsurface magma reservoir, or lava pond, which also sourced low viscosity material that flooded local topographic lows.

[60] Distinctive ribbon-tessera terrain represents lava pond "scum," a competent surface layer that congeals across the lava pond with an areal extent similar to that of an individual crustal plateau. Folds form by selective amplification of instabilities in the congealed surface as a result of layer shortening, likely driven by convection in the magma. Extensional structures form with trends normal to fold crests, tracking maximum horizontal extension. Subsurface magma variably leaks to the surface as lava, flooding local lows in structural topography and solidifying. With time the surface layer thickens as a result of deformation (principally horizontal contraction resulting in layer thickening), cooling and resulting growth of the solid layer as the solidus isotherm migrates downward, and through local flooding and subsequent solidification of lava within structural lows. As the surface layer thickened, longer wavelength contractional and extensional structures formed.

[61] Lava pond formation could result from massive partial melting in the shallow ductile mantle as a result of either, the impact of a large bolide on ancient thin lithosphere, or a large mantle plume. Bolide impact is favored herein. In either case, melt rises to the surface buoyantly to form a lava pond, leaving behind a lens of low-density mantle residuum. Isostatic adjustment resulting from the residuum raises the solidified lava pond to plateau stature. Later, mantle convection processes could strip away the low-density residuum lens, leading to plateau subsidence or collapse; or, secular cooling could result in an increase in the thickness of the lithosphere globally, trapping the residuum lens and preserving the lava pond as a high-standing crustal plateau. Thin surface deposits could partially or completely covered the distinctive pond scum fabrics of collapsed plateaus, obscuring or erasing, the record of some ancient lava ponds. The bolide-induced lava-pond hypothesis for crustal plateau formation could provide a mechanism for spatially punctuated equilibrium resurfacing as long as Venus had a lithosphere thin enough to allow massive partial melting of the mantle as a result of large bolide impact. As Venus' lithosphere thickened with secular cooling (presumably >30–50 km thickness), large bolides that impacted the surface would no longer cause partial melting and instead form large impact basins such as Mead Crater instead.

[62] **Acknowledgments.** This work was supported by NASA grants NNG04GG36G and NAG5-13432 to Hansen and the University of Minnesota Duluth and by the McKnight Foundation. Discussions with, and comments by, R. Bannister, J. Goodge, T. Gregg, I. Lopez, N. Lang, and J. Swenson were extremely helpful. Careful, thorough, and thoughtful reviews by L. Montési and an anonymous reviewer greatly improved the contribution.

References

Aubele, J. (1996), Akkruva small shield plains: Definition of a significant regional plains unit on Venus, *Lunar Planet. Sci.*, *XXVII*, 49–50.
Banerdt, W. B., G. E. McGill, and M. T. Zuber (1997), Plains tectonics on Venus, in *Venus II*, edited by S. W. Bouger et al., pp. 901–930, Univ. of Ariz. Press, Tucson.
Banks, B. K., and V. L. Hansen (2000), Relative timing of crustal plateau magmatism and tectonism at Tellus, Regio, Venus, *J. Geophys. Res.*, *105*(E7), 17,655–17,667.
Basilevsky, A. T., and J. W. Head III (1998), The geologic history of Venus: A stratigraphic view, *J. Geophys. Res.*, *103*(E4), 8531–8544.
Bercovici, D., and J. Mahoney (1994), Double flood basalts and plume head separation at the 660-kilometer discontinuity, *Science*, *266*, 1367–1369.
Bindschadler, D. L. (1995), Magellan: A new view of Venus' geology and geophysics, *Rev. Geophys.*, *33*(S1), 459–467.
Bindschadler, D. L., and J. W. Head (1991), Tessera terrain, Venus: Characterization and models for origin and evolution, *J. Geophys. Res.*, *96*(B4), 5889–5907.
Bindschadler, D. L., and E. M. Parmentier (1990), Mantle flow tectonics: The influence of a ductile lower crust and implications for the formation of topographic uplands on Venus, *J. Geophys. Res.*, *95*(B13), 21,329–21,344.

Bindschadler, D. L., G. Schubert, and W. M. Kaula (1992a), Coldspots and hotspots: Global tectonics and mantle dynamics of Venus, *J. Geophys. Res.*, *97*(E8), 13,495–13,532.

Bindschadler, D. L., A. deCharon, K. K. Beratan, S. E. Smrekar, and J. W. Head (1992b), Magellan observations of Alpha Regio: Implications for formation of complex ridged terrains on Venus, *J. Geophys. Res.*, *97*(E8), 13,563–13,577.

Biot, M. A. (1961), Theory of folding of stratified visco-elastic media and its implications in tectonics and orogenesis, *Geol. Soc. Am. Bull.*, *72*, 1595–1620.

Braun, M. G., G. Hirth, and E. M. Parmentier (2000), The effects of deep damp melting on mantle flow and melt generation beneath mid-ocean ridges, *Earth Planet. Sci. Lett.*, *176*, 339–356.

Brown, C. D., and R. E. Grimm (1997), Tessera deformation and the contemporaneous thermal state of the plateau highlands, Venus, *Earth Planet. Sci. Lett.*, *147*, 1–10.

Brown, C. D., and R. E. Grimm (1999), Recent tectonic and lithospheric thermal evolution of Venus, *Icarus*, *139*, 40–48.

Campbell, B. A. (1999), Surface formation rates and impact crater densities on Venus, *J. Geophys. Res.*, *104*(E9), 21,951–21,955.

Chamberlin, T. C. (1897), The method of multiple working hypotheses, *J. Geol.*, *5*, 837–848.

Choblet, G., and E. M. Parmentier (2001), Mantle upwelling and melting beneath slow spreading centers: Effects of variable rheology and melt productivity, *Earth Planet. Sci. Lett.*, *184*, 589–604.

Coffin, M. F., and O. Eldholm (1994), Large igneous provinces: Crustal structure, dimensions, and external consequences, *Rev. Geophys.*, *32*(1), 1–36.

DeShon, H. R., D. A. Young, and V. L. Hansen (2000), Geologic evolution of southern Rusalka Planitia, Venus, *J. Geophys. Res.*, *105*(E3), 6983–6995.

Elkins-Tanton, L., and B. Hager (2005), Giant meteoroid impacts can cause volcanism, *Earth Planet. Sci. Lett.*, *239*, 219–232.

Farnetani, C. G., and M. A. Richards (1994), Numerical investigations of the mantle plume initiation model for flood basalt events, *J. Geophys. Res.*, *99*(B17), 13,813–13,833.

Farnetani, C. G., M. A. Richards, and M. S. Ghiorso (1996), Petrological models of magma evolution and deep crustal structure beneath hotspots and flood basalt provinces, *Earth Planet. Sci. Lett.*, *143*, 81–92.

Fink, J. H., and R. C. Fletcher (1978), Ropy pahoehoe: Surface folding of a viscous fluid, *J. Volcanol. Geotherm. Res.*, *4*, 151–170.

Fletcher, R. C. (1974), Wavelength selection in the folding of a single layer with power-law rheology, *Am. J. Sci.*, *274*, 1029–1043.

Ford, J. P., J. J. Plaut, C. M. Weitz, T. G. Farr, D. A. Senske, E. R. Stofan, G. Michaels, and T. J. Parker (1993), Guide to Magellan image interpretation, *JPL Publ.*, *93-24*, 148 pp.

Ghail, R. C. (2002), Structure and evolution of southeast Thetis Regio, *J. Geophys. Res.*, *107*(E8), 5060, doi:10.1029/2001JE001514.

Ghent, R. R., and V. L. Hansen (1999), Structural and kinematic analysis of eastern Ovda Regio, Venus: Implications for crustal plateau formation, *Icarus*, *139*, 116–136.

Ghent, R. R., and I. M. Tibuleac (2002), Ribbon spacing in Venusian tessera: Implications for layer thickness and thermal state, *Geophys. Res. Lett.*, *29*(20), 2000, doi:10.1029/2002GL015994.

Ghent, R. R., R. J. Phillips, V. L. Hansen, and D. C. Nunes (2005), Finite element modeling of short-wavelength folding on Venus: Implications for the plume hypothesis for crustal plateau formation, *J. Geophys. Res.*, *110*, E11006, doi:10.1029/2005JE002522.

Gilbert, G. K. (1886), Inculcation of the scientific method, *Am. J. Sci.*, *31*, 284–299.

Gilmore, M. S., and J. W. Head (2000), Sequential deformation of plains at the margins of Alpha Regio, Venus: Implications for tessera formation, *Meteor. Planet. Sci.*, *35*, 667–687.

Gilmore, M. S., M. A. Ivanov, J. W. Head III, and A. T. Basilevsky (1997), Duration of tessera deformation on Venus, *J. Geophys. Res.*, *102*(E6), 13,357–13,368.

Gilmore, M. S., G. C. Collins, M. A. Ivanov, L. Marinangeli, and J. W. Head (1998), Style and sequence of extensional structures in tessera terrain, Venus, *J. Geophys. Res.*, *103*(E7), 16,813–16,840.

Gregg, T. K. P., J. H. Fink, and R. W. Griffiths (1998), Formation of multiple fold generations on lava flow surfaces: Influence of strain rate, cooling rate, and lava composition, *J. Volcanol. Geotherm. Res.*, *80*, 281–292.

Griffiths, R. W., M. Gurnis, and G. Eitelberg (1989), Holographic measurements of surface topography in laboratory models of mantle hotspots, *Geophys. J.*, *96*, 477–495.

Grimm, R. E. (1994a), The deep structure of Venusian plateau highlands, *Icarus*, *112*, 89–103.

Grimm, R. E. (1994b), Recent deformation rates on Venus, *J. Geophys. Res.*, *99*(E11), 23,163–23,171.

Hamilton, W. B. (2005), Plumeless Venus has ancient impact-accretionary surface, in *Plates, Plumes, and Paradigms*, edited by G. R. Foulger et al., *Spec. Pap. Geol. Soc. Am.*, *388*, 781–814.

Hansen, V. L. (1992), Regional non-coaxial deformation on Venus: Evidence from western Itzapapalotl tessera, *Lunar Planet. Sci.*, *XXIII*, 479–480.

Hansen, V. L. (2000), Geologic mapping of tectonic planets, *Earth Planet. Sci. Lett.*, *176*, 527–542.

Hansen, V. L. (2002), Artemis: Signature of a deep Venusian mantle plume, *Geol. Soc. Am. Bull.*, *114*, 839–848.

Hansen, V. L. (2003), Venus diapirs: Thermal or compositional?, *Geol. Soc. Am. Bull.*, *115*, 1040–1052.

Hansen, V. L. (2005a), Venus's shield-terrain, *Geol. Soc. Am. Bull.*, *117*, 808–822.

Hansen, V. L. (2005b), SPatially Isolated Time-Transgressive Equilibrium Resurfacing: The SPITTER hypothesis, an alternative to catastrophic resurfacing of Venus, *Geol. Soc. Am. Abstr. Prog.*, *37*(7), 36-2.

Hansen, V. L. (2006a), Geologic map of the Niobe Planitia quadrangle (V-23), Venus, 1:5M scale, map, U.S. Geol. Surv., Boulder, Colo., in press.

Hansen, V. L. (2006b), LIPs on Venus, *Chem. Geol.*, in press.

Hansen, V. L., and L. F. Bleamaster III (2002), Distributed point source volcanism: A mechanism for 'regional plains' resurfacing Venus, *Lunar Planet Sci.*, *XXXIII*, abstract 1061.

Hansen, V. L., and J. J. Willis (1996), Structural analysis of a sampling of tesserae: Implications for Venus geodynamics, *Icarus*, *123*, 296–312.

Hansen, V. L., and J. J. Willis (1998), Ribbon terrain formation, southwestern Fortuna Tessera, Venus: Implications for lithosphere evolution, *Icarus*, *132*, 321–343.

Hansen, V. L., and D. A. Young (2006), Venus evolution: A synthesis, in *Convergent Margin Terranes and Associated Regions: A Tribute to W. G. Ernst*, edited by M. Cloos et al., *Spec. Pap. Geol. Soc. Am.*, in press.

Hansen, V. L., J. J. Willis, and W. B. Banerdt (1997), Tectonic overview and synthesis, in *Venus II: Geology, Geophysics, Atmosphere, and Solar Wind Environment*, edited by S. W. Bougher, D. M. Hunten, and R. J. Phillips, pp. 797–844, Univ. of Ariz. Press, Tucson.

Hansen, V. L., B. K. Banks, and R. R. Ghent (1999), Tessera terrain and crustal plateaus, Venus, *Geology*, *27*, 1071–1074.

Hansen, V. L., R. J. Phillips, J. J. Willis, and R. R. Ghent (2000), Structures in tessera terrain: Issues and answers, *J. Geophys. Res.*, *105*(E2), 4135–4152.

Head, J. W., and A. T. Basilevsky (1998), Sequence of tectonic deformation in the history of Venus: Evidence from global stratigraphic relationships, *Geology*, *26*, 35–38.

Huddleston, P., and L. Lan (1995), Rheological information from geological structures, *Pure Appl. Geophys.*, *145*, 607–620.

Ignacio, R., C. Ramón, and A. Francisco (2005), Tectonic and kinematic study of a strike-slip zone along the southern margin of Central Ovda Regio, Venus: Geodynamical implications for crustal plateaux formation and evolution, *Icarus*, *175*, 320–334.

Ingle, S., and M. F. Coffin (2004), Impact origin for the greater Ontong Java Plateau?, *Earth Planet. Sci. Lett.*, *218*, 123–134.

Ito, G., and P. D. Clift (1998), Subsidence and growth of Pacific Cretaceous plateaus, *Earth Planet. Sci. Lett.*, *161*, 85–99.

Ito, G., and A. Taira (2000), Compensation of the Ontong Java Plateau by surface and subsurface loading, *J. Geophys. Res.*, *105*(B5), 11,171–11,183.

Ivanov, M. A., and J. W. Head (1996), Tessera terrain on Venus: A survey of the global distribution, characteristics, and relation to surrounding units from Magellan data, *J. Geophys. Res.*, *101*(E6), 14,861–14,908.

Ivanov, M. A., and J. W. Head (2003), Evolution of three largest coronae on Venus, Heng-O, Quetzalpetlatl, and Artemis: Preliminary results, *Lunar Planet. Sci. Conf.*, *XXXIV*, abstract 1188.

Ivanov, B. A., and H. J. Melosh (2003), Impacts do not initiate volcanic eruptions, *Geology*, *31*, 869–872.

Jha, K., E. M. Parmentier, and J. Phipps-Morgan (1994), The role of mantle-depletion and melt-retention buoyancy in spreading-center segmentation, *Earth Planet. Sci. Lett.*, *125*, 221–234.

Jones, A. P., G. D. Price, N. J. Price, P. S. DeCarli, and R. A. Clegg (2002), Impact induced melting and the development of large igneous provinces, *Earth Planet. Sci. Lett.*, *202*, 551–561.

Jones, A. P., K. Wunemann, and D. Price (2005), Impact volcanism as a possible origin for the Ontong Java Plateau (OJP), in *Plates, Plumes, and Paradigms*, edited by G. R. Foulger et al., *Spec. Pap. Geol. Soc. Am.*, *388*, 711–720.

Jordan, T. H. (1975), The continental tectosphere, *Rev. Geophys.*, *13*(3), 1–12.

Jordan, T. H. (1981), Continents as a chemical boundary layer, *Philos. Trans. R. Soc., Ser. A*, *301*, 359–373.

Kidan, T. W., and J. W. Cosgrove (1996), The deformation of multilayers by layer-normal compression: An experimental investigation, *J. Struct. Geol.*, *18*, 461–678.

Kidder, J. G., and R. J. Phillips (1996), Convection-driven subsolidus crustal thickening on Venus, *J. Geophys. Res.*, *101*(E10), 23,181–23,294.

Kiefer, W. S., and K. Peterson (2003), Mantle and crustal structure in Phoebe Regio and Devana Chasma, Venus, *Geophys. Res. Lett.*, *30*(1), 1005, doi:10.1029/2002GL015762.

Kirk, R., L. Soderblom, and E. Lee (1992), Enhanced visualization for interpretation of Magellan radar data: Supplement to the Magellan special issue, *J. Geophys. Res.*, *97*(E10), 16,371–16,380.

Kobberger, G., and G. Zulauf (1995), Experimental folding and boudinage under pure constructional conditions, *J. Struct. Geol.*, *17*, 1055–1063.

Kumar, P. S. (2005), An alternative kinematic interpretation of Thetis Boundary Shear Zone, Venus: Evidence for strike-slip ductile duplexes, *J. Geophys. Res.*, *110*, E07001, doi:10.1029/2004JE002387.

Lang, N. P., and V. L. Hansen (2005), Geologic map of the Greenaway quadrangle (V-24), Venus, 1:5M scale, map, U.S. Geol. Surv., Boulder, Colo., in revision.

Mackwell, S. J., M. E. Zimmerman, and D. L. Kohlstedt (1998), High-temperature deformation of dry diabase with application to tectonics on Venus, *J. Geophys. Res.*, *103*(B1), 975–984.

McGill, G. E. (1994), Hotspot evolution and Venusian tectonic style, *J. Geophys. Res.*, *99*(E11), 23,149–23,161.

McKinnon, W. B., K. J. Zahnle, B. A. Ivanov, and H. J. Melosh (1997), Cratering on Venus: Models and observations, in *Venus II*, edited by S. W. Bougher, D. M. Hunten, and R. J. Phillips, pp. 969–1014, Univ. of Ariz. Press, Tucson.

Mege, D., A. C. Cook, E. Garel, Y. Lagabrielle, and M. H. Cormier (2003), Volcanic rifting at Martian grabens, *J. Geophys. Res.*, *108*(E5), 5044, doi:10.1029/2002JE001852.

Montési, L. G. J., and M. T. Zuber (2003), Spacing of faults at the scale of the lithosphere and localization instability: 1. Theory, *J. Geophys. Res.*, *108*(B2), 2110, doi:10.1029/2002JB001923.

Nimmo, F., and D. McKenzie (1998), Volcanism and tectonics on Venus, *Annu. Rev. Earth Planet. Sci.*, *26*, 23–52.

Nunes, D. C., R. J. Phillips, C. D. Brown, and A. J. Dombard (2004), Relaxation of compensated topography and the evolution of crustal plateaus on Venus, *J. Geophys. Res.*, *109*, E01006, doi:10.1029/2003JE002119.

Okubo, C. H., and S. J. Martel (1998), Pit crater formation on Kilauea volcano, Hawaii, *J. Volcanol. Geotherm. Res.*, *86*, 1–8.

Phillips, R. J., and V. L. Hansen (1994), Tectonic and magmatic evolution of Venus, *Annu. Rev. Earth Planet. Sci.*, *22*, 597–656.

Phillips, R. J., and V. L. Hansen (1998), Geological evolution of Venus: A geodynamical and magmatic framework, *Science*, *279*, 1492–1497.

Phillips, R. J., R. E. Grimm, and M. C. Malin (1991), Hot-spot evolution and the global tectonics of Venus, *Science*, *252*, 651–658.

Plaut, J. J. (1993), Stereo imaging, in *Guide to Magellan Image Interpretation*, edited by J. P. Ford et al., *JPL Publ.*, *93-24*, 33–41.

Price, N. J. (2001), *Major Impacts and Plate Tectonics: A Model for the Phanerozoic Evolution of the Earth's Lithosphere*, 354 pp., Routledge, Boca Raton, Fla.

Price, N., and J. Cosgrove (1990), *Analysis of Geological Structures*, 502 pp., Cambridge Univ. Press, New York.

Pritchard, M. E., V. L. Hansen, and J. J. Willis (1997), Structural evolution of western Fortuna Tessera, Venus, *Geophys. Res. Lett.*, *24*(18), 2339–2342.

Raitala, J., and M. Black (1996), Tectonics of small tessera islets on Venus, *Planet. Space Sci.*, *44*, 843–857.

Ramberg, H. (1962), Contact strain and folding instability of a multilayered body under compression, *Geol. Rundsch.*, *51*, 405–439.

Reese, C. C., V. S. Solomatov, J. R. Baumgardner, D. R. Stegman, and A. V. Vezolainen (2004), Magmatic evolution of impact-induced Martian mantle plumes and the origin of Tharsis, *J. Geophys. Res.*, *109*, E08009, doi:10.1029/2003JE002222.

Rogers, G. C. (1982), Oceanic plateaus as meteorite impact signatures, *Nature*, *299*, 341–342.

Romeo, I., R. Capote, and F. Anguita (2005), Tectonic and kinematic study of a strike-slip zone along the southern margin of Central Ovda Regio, Venus: Geodynamical implications for crustal plateaux formation and evolution, *Icarus*, *175*, 320–334.

Schubert, G. S., V. S. Solomatov, P. J. Tackely, and D. L. Turcotte (1997), Mantle convection and thermal evolution of Venus, in *Venus II*, edited by S. W. Bougher, D. M. Hunten, and R. J. Phillips, pp. 1245–1288, Univ. of Ariz. Press, Tucson.

Senske, D. A. (1999), Geology of the Tellus Tessera quadrangle (V-10), Venus, *Proc. Lunar Planet. Sci. Conf.*, *XXXth*, 1668–1669.

Sherwin, J., and W. M. Chapple (1968), Wavelengths of single layer folds: A comparison between theory and observation, *Am. J. Sci.*, *266*, 167–179.

Simons, M., S. C. Solomon, and B. H. Hager (1997), Localization of gravity and topography: Constraints on the tectonics and mantle dynamics of Venus, *Geophys. J. Int.*, *131*, 24–44.

Smith, R. B. (1975), Unified theory of the onset of folding, boudinage, and mullion structure, *Geol. Soc. Am. Bull.*, *86*, 1601–1609.

Smith, R. B. (1977), Formation of folds, boudinage and mullions in non-Newtonian materials, *Geol. Soc. Am. Bull.*, *88*, 312–320.

Smrekar, S. E., and R. J. Phillips (1991), Venusian highlands: Geoid to topography ratios and their implications, *Earth Planet. Sci. Lett.*, *107*, 582–597.

Smrekar, S. E., and E. R. Stofan (1997), Corona formation and heat loss on Venus by coupled upwelling and delamination, *Science*, *277*, 1289–1294.

Smrekar, S. E., W. S. Kiefer, and E. R. Stofan (1997), Large volcanic rises on Venus, in *Venus II*, edited by S. W. Bougher, D. M. Hunten, and R. J. Phillips, pp. 845–879 Univ. of Ariz. Press, Tucson.

Snyder, D. (2002), Cooling of lava flows on Venus: The coupling of radiative and convective heat transfer, *J. Geophys. Res.*, *107*(E10), 5080, doi:10.1029/2001JE001501.

Solomatov, V. S., and L. N. Moresi (1996), Stagnant lid convection on Venus, *J. Geophys. Res.*, *101*(E2), 4737–4753.

Solomon, S. C. (1993), The geophysics of Venus, *Phys. Today*, *46*, 48–55.

Stofan, E. R., D. A. Senske, and G. Michaels (1993), Tectonic features in Magellan data, in *Guide to Magellan Image Interpretation*, edited by J. P. Ford et al., *JPL Publ.*, *93-24*, 93–108.

Talbot, C. J. (1970), The minimum strain ellipsoid using deformed quartz veins, *Tectonophysics*, *9*, 47–76.

Tanaka, K. L., et al. (1994), *The Venus Geologic Mappers' Handbook*, 2nd ed., *U.S. Geol. Surv. Open File Rep.*, *94-438*, 52 pp.

Tapponnier, P., G. Peltzer, A. Y. Le Dain, R. Armijo, and P. Cobbold (1982), Propagating extrusion tectonics in Asia: New insights from simple experiments with plasticine, *Geology*, *10*, 611–616.

Tarduno, J. A., W. V. Sliter, L. Kroenke, M. Leckie, H. Mayer, J. Mahoney, R. Musgrave, M. Storey, and E. L. Winterer (1991), Rapid formation of Ontong Java Plateau by Aptian mantle plume volcanism, *Science*, *254*, 399–403.

Tuckwell, G. W., and R. C. Ghail (2003), A 400-km-scale strike-slip zone near the boundary of Thetis Regio, Venus, *Earth Planet. Sci. Lett.*, *211*, 45–55.

Wilhelms, D. E. (1990), Geologic mapping, in *Planetary Mapping*, edited by R. Greeley and R. M. Batson, pp. 208–260, Cambridge Univ. Press, New York.

Zimbelman, J. R. (2001), Image resolution and evaluation of genetic hypotheses for planetary landscapes, *Geomorphology*, *37*, 179–199.

Zuber, M. T., and E. M. Parmentier (1996), Finite amplitude folding of continuously viscosity-stratified lithosphere, *J. Geophys. Res.*, *101*(B3), 5489–5498.

V. L. Hansen, Department of Geological Sciences, University of Minnesota at Duluth, Duluth, MN 55812, USA. (vhansen@d.umn.edu)